AD-A112 190 AERONAUTICAL RESEARCH LABS MELBOURNE (AUSTRALIA) F/G 20/4
A NUMERICAL INVESTIGATION OF TWO-DIMENSIONAL, SUBSONIC, LINEAR,--ETC(U)
JUN 81 N POLLOCK
UNCLASSIFIED ARL/AERO NOTE-403 NL

1 OF 1
AD A
12190

END
DATE
FILMED
04-82
DTIC

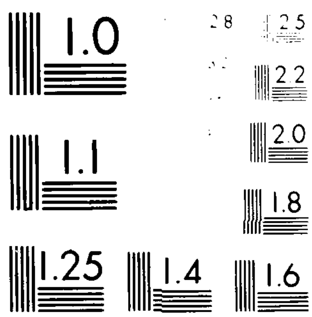
1.0
2.5
2.2
2.0
1.1
1.8
1.25
1.4
1.6

(12)

ARL-AERO-NOTE-403

AR-002-294

AUSTRALIA

ADA112190

DEPARTMENT OF DEFENCE

DEFENCE SCIENCE AND TECHNOLOGY ORGANISATION

AERONAUTICAL RESEARCH LABORATORIES

MELBOURNE, VICTORIA

AERODYNAMICS NOTE 403

A NUMERICAL INVESTIGATION OF TWO-DIMENSIONAL, SUBSONIC, LINEAR, WIND TUNNEL INTERFERENCE THEORY

by

N. POLLOCK

Approved for Public Release.

A

COPY No

JUNE 1981

AR-002-294

DEPARTMENT OF DEFENCE
DEFENCE SCIENCE AND TECHNOLOGY ORGANISATION
AERONAUTICAL RESEARCH LABORATORIES

AERODYNAMICS NOTE 403

A NUMERICAL INVESTIGATION OF TWO-DIMENSIONAL, SUBSONIC, LINEAR, WIND TUNNEL INTERFERENCE THEORY

by

N. POLLOCK

SUMMARY

An investigation of two-dimensional, subsonic, linear wind tunnel interference using the computer program TSFOIL as a "numerical tunnel" has been carried out for solid, open, porous and slotted walls. The use of a computer code rather than physical experiment has the advantage that test parameters such as wall characteristics and model chord can be varied widely at low cost.

The aim of the investigation was to determine the relative merits of the various walls and to establish the limits of applicability of linear interference theory. The most favourable wall type was found to be an ideal slotted wall with the slot parameter appropriate for zero solid blockage ($F = 1 \cdot 1844$). For this wall type linear interference theory accurately predicted lift and pitching moment corrections for tunnel height to chord ratios greater than 2 and supersonic region height to tunnel height ratios less than $0 \cdot 2$.

POSTAL ADDRESS: Chief Superintendent, Aeronautical Research Laboratories, Box 4331, P.O., Melbourne, Victoria, 3001, Australia.

DOCUMENT CONTROL DATA SHEET

Security classification of this page: Unclassified

1. Document Numbers
   (a) AR Number
   AR-002-294
   (b) Document Series and Number:
   Aerodynamics Note 403
   (c) Report Number:
   ARL-Aero-Note-403

2. Security Classification
   (a) Complete document:
   Unclassfied
   (b) Title in isolation:
   Unclassified
   (c) Summary in isolation:
   Unclassified

3. Title: A NUMERICAL INVESTIGATION OF TWO-DIMENSIONAL, SUBSONIC, LINEAR WIND TUNNEL INTERFERENCE THEORY

4. Personal Author:
   N. Pollock

5. Document Date:
   June 1981

6. Type of Report and Period Covered:

7. Corporate Author(s):
   Aeronautical Research Laboratories

8. Reference Numbers
   (a) Task:
   DST 79/107
   (b) Sponsoring Agency:
   DSTO

9. Cost Code:
   547710

10. Imprint:
   Aeronautical Research Laboratories, Melbourne

11. Computer Program(s) (Title(s) and language(s)):
   TSFOIL

12. Release Limitations (of the document): Approved for Public Release

12-0. Overseas:	N.O.		P.R.	1	A		B		C		D		E	

13. Announcement Limitations (of the information on this page): No Limitations

14. Descriptors:
   Wall Interference
   Subsonic Wind Tunnels
   Two-Dimensional Flow

15. Cosati Codes:
   1402
   2004
   0101

16.

ABSTRACT

An investigation of two-dimensional, subsonic, linear wind tunnel interference using the computer program TSFOIL as a "numerical tunnel" has been carried out for solid, open, porous and slotted walls. The use of a computer code rather than physical experiment has the advantage that test parameters such as wall characteristics and model chord can be varied widely at low cost.

The aim of the investigation was to determine the relative merits of the various walls and to establish the limits of applicability of linear interference theory. The most favourable wall type was found to be an ideal slotted wall with the slot parameter appropriate for zero solid blockage (F   1·1844). For this wall type linear interference theory accurately predicted lift and pitching moment corrections for tunnel height to chord ratios greater than 2 and supersonic region height to tunnel height ratios less than 0·2.

CONTENTS

NOTATION

a	Tunnel wall slot width
A	Cross-sectional area of model
c	Model chord
C_L	Lift coefficient $=$ Lift$/\frac{1}{2}\rho U^2 S$
C_m	Pitching moment coefficient $=$ Pitching moment about $c/4/\frac{1}{2}\rho U^2 Sc$
C_D	Drag coefficient $=$ Drag$/\frac{1}{2}\rho U^2 S$
C_p	Pressure coefficient $=$ (local pressure—free stream static pressure)$/\frac{1}{2}\rho U^2$
F	Non-dimensional wind tunnel slot parameter $= \frac{2s}{\pi h} \ln \operatorname{cosec}\left(\frac{\pi a}{2s}\right)$
h	Tunnel height
M	Mach number
P	Porosity factor
s	Distance between slot centres
S	Model area (chord $\times$ span)
t	Model thickness
U	Free stream velocity
α	Model incidence
β	$\sqrt{1 - M^2}$
ρ	Free stream density

Subscript

c	corrected values

1. INTRODUCTION

During the last 15 years there have been very rapid advances in the numerical calculations of fluid flows and this has raised questions regarding the future role of wind tunnels for aerodynamic testing. However, the very extensive review of computation and tunnel testing presented in Reference 1 concludes that "For the foreseeable future computers and wind tunnels will be complementary".

An example of this complementary relationship can be seen in the current development of self streamlining tunnels[2] where a computer is used to modify the test section walls so that they resemble streamlines in an unconfined flow thus reducing wall interference. At the present rate of development the first production tunnel to use self streamlining walls would seem to be some years away. Even when the technology is proved many smaller tunnels will probably not be fitted with self streamlining walls due to the expense of the computer and wall modifying system required. In view of the probable slow rate of construction of self streamlining tunnels it is worthwhile considering ways in which modern developments in numerical fluid mechanics can be used to support the operation of existing conventional facilities.

Since the 1930s low-speed wind tunnels have used corrections based on linear theory[3] to account for the effects of tunnel wall interference in closed or open jet test sections. Following the introduction of transonic wind tunnels with slotted or porous test sections, linear interference theory was extended[3] to include these wall types. Over the years a considerable body of empirical knowledge has been built up concerning the accuracy and limits of applicability of linear interference theory. However, particularly at high subsonic and transonic speeds, there are still many uncertainties in the use of the theory.

In this Note an investigation into the accuracy and limitations of linear interference theory using the two-dimensional, transonic small disturbance computer program TSFOIL[4,5] is presented. The use of a computer code rather than physical experiment has the major advantage that the test parameters (e.g. model chord, wall open area ratio) can be varied much more widely than would otherwise be practical. The absence of viscous effects in the computation also removes one of the variables which tends to obscure wall interference effects in physical experiments.

2. DESCRIPTION OF METHOD

The basic method adopted for this investigation was as follows: For a particular aerofoil section, Mach number and incidence the free air lift, drag and pitching moment coefficients were calculated using TSFOIL. For the same nominal test conditions and a selected tunnel wall type, calculations of aerofoil characteristics over a range of h/c ratios were carried out. The errors introduced by the tunnel walls were obtained by comparing the tunnel and free air computed values of C_L and C_m. C_D values were not used in the comparison for reasons discussed in the next section. The simulated tunnel results were then corrected to the equivalent free air values using linear subsonic interference theory. Free air computations were then carried out at the corrected values of α and M for each of the tunnel cases. The residual errors in the corrected results were obtained by comparing the corrected tunnel computed values with the free air values calculated at the corrected values of α and M.

The C_L errors are presented as a percentage since in this form their magnitude is most readily appreciated. The C_m errors are presented as absolute values since a percentage presentation is not easily understood when the reference magnitude of the variable (and also its sign) varies widely.

Aerofoil sections 6% and 12% thick were used since they are near the limits of thickness/chord ratio of major current interest. The computations were carried out at low angles of incidence (mostly at 2°) since the small disturbance approximations used in TSFOIL would give increasing

errors at higher angles. The use of low angles of incidence also ensured that both blockage and lift interference effects were significant so an assessment of all aspects of the linear interference theory could be carried out without requiring the computation of an excessive number of cases.

For the above procedure to give a reliable indication of the accuracy of linear interference theory it is necessary that *TSFOIL* be considerably more accurate than the interference theory being assessed. There is strong evidence available to indicate that this condition is met. TSFOIL uses a mathematical formulation of a considerably higher order of approximation to the full equations of motion than does the linear interference theory. Comparisons between TSFOIL computations and the results of experiments and other computational methods[4] give considerable confidence in the ability of the code to accurately predict unconstrained free air results. Although there is little direct evidence of the accuracy of TSFOIL in predicting constrained tunnel results, the nature of the program and the way in which the boundary conditions are applied strongly suggests that tunnel results will have the same order of accuracy as free air results.

Some problems with convergence and subcritical drag prediction were experienced with TSFOIL during this investigation. However, it is considered that these problems do not affect the accuracy of the overall conclusions.

A listing of all computed results is included in the Appendix.

2.1 Computer Program

The program TSFOIL was chosen for this investigation since it was a readily available (a listing appears in Reference 5) well proven code which included tunnel wall conditions. A number of more accurate and efficient programs are available for the calculation of free air aerofoil flows (e.g. Ref. 6) but since they are all solved in a transformed plane rather than in the physical plane the application of tunnel wall boundary conditions is much more difficult.

The computational grid included in the program extended from 1·075c upstream of the aerofoil leading edge to 0·875c downstream of the trailing edge. To produce a more realistic test section length for tunnel simulation the grid was extended to 4·575c upstream of the leading edge and 4·375c downstream of the trailing edge. To achieve this grid extension the values −4·575, −4·075, −3·575, −3·075, −2·575, −2·075, −1·575, −1·325, 2·125, 2·375, 2·875, 3·375, 3·875, 4·375, 4·875 and 5·375 were added to the array XKRUPP and the variable IMAXI was increased to 93. Both these changes were made in the block data subprogram. The extended grid was also used for all free air calculations. This grid extension slightly reduced the rate of convergence and most cases required from 15 to 20 minutes on the ARL DEC system 10 computer.

When convergence was not obtained after 750 iterations on the fine grid the computation was terminated and the trends of C_L and C_m examined. If they had settled to constant values they were used and if not the computation was discarded.

The drag coefficients calculated by TSFOIL were viewed with caution since some subcritical (and therefore hopefully drag free) computations produced significant drag values. Due to this problem, drag coefficients were not used in the interference comparisons. However, the computed supercritical drag coefficients were used as inputs to the interference correction scheme described in the next section. It was considered that this was more desirable than simply omitting the blockage correction due to wave drag. For subcritical cases a drag coefficient of zero was used in the correction scheme.

2.2 Linear Interference Theory

The linear interference theory presented in Reference 3, and more recently, with corrections, in References 7 and 8 was used to correct the simulated tunnel results. A concise summary of the correction scheme as used in this investigation is presented below:

$$\alpha_c = \alpha + \delta_0\left(\frac{c}{h}\right)C_L + \frac{\delta_1}{\beta}\left(\frac{c}{h}\right)^2\left(\frac{C_L}{4} + C_m\right)$$

$$M_c = M[1 + (1 + 0.2M^2)\epsilon_B]$$

$$C_{L_c} = C_L\left[1 - \frac{\pi}{2}\cdot\frac{\delta_1}{\beta^2}\cdot\left(\frac{c}{h}\right)^2\right]G$$

$$C_{m_c} = \left[C_m + \frac{\pi}{8}\cdot\frac{\delta_1}{\beta^2}\cdot\left(\frac{c}{h}\right)^2 C_L\right]G$$

where

$$G = \frac{1}{1 + (2 - M^2)\epsilon_B}$$

$$\epsilon_B = \frac{\Omega_s \pi A}{6\beta^3 h^2}\left[1 + 1\cdot2\beta\left(\frac{t}{c}\right)\right]\left[1 + 1\cdot1\left(\frac{c}{t}\right)\alpha^2\right] + \frac{\Omega_w}{4}\left(\frac{c}{h}\right)\frac{(1 + 0\cdot4M^2)}{\beta^2}C_D$$

The values of the parameters δ_0, δ_1, Ω_s and Ω_w used for the various tunnel conditions considered in this investigation are presented in the following table. The values were obtained from References 7 and 8.

Wall type	δ_0	δ_1	Ω_s	Ω_w
Solid	0	0·1309	1·0	1·0
Open jet	0·25	0·2618	−0·5	0
Porous ($\beta P = 0{\cdot}78$)	0·144	0	−0·23	0·42
Slotted ($F = 1{\cdot}59$)	0	0	0·078	0
Slotted ($F = 1{\cdot}1844$)	0	0·025	0	0

The downwash parameter δ_0 for the slotted walls was set at zero instead of the finite values given in References 7 and 8 because the downwash term $\frac{cC_L}{4h(1 + F)}$ introduced by Wright[9] was not included in the boundary conditions used in TSFOIL. The zero value of δ_0 exactly cancels the effect of the missing downwash term and the accuracy of the error comparisons is not affected.

3. RESULTS AND DISCUSSION

3.1 Solid Walls

The first tunnel type studied was the simple solid wall test section. This is a case of considerable practical importance since many low-speed tests are conducted in sold wall tunnels. The mathematical formulation of the boundary conditions for these walls is quite straightforward and, apart from a small discrepancy due to tunnel wall boundary layers, the theoretical predictions should give a good indication of the real interference effects observed in tunnel tests.

A series of calculations were carried out on NACA 0006, NACA 0012 and 12 % symmetrical parabolic aerofoils at a Mach number of 0·55. This Mach number was selected because compressibility effects would be significant but the simple compressibility corrections used in the linear interference theory should adequately account for them. A comparison of uncorrected and corrected C_L errors for the above cases is presented in Figure 1. From this figure it can be seen that both the uncorrected and corrected C_L errors form approximately universal curves when plotted against h/c. An h/c value of about 3 appears to be a useful lower limit if the corrected C_L values are to be accurate to 1 %. Corrected and uncorrected C_m errors are plotted in Figure 2. The corrected errors again fall on an approximately universal curve and a minimum safe value for h/c from a C_m point of view appears to be about 2·5. It is interesting to note that practical experience[8] suggests a minimum practical h/c value of about 2·9.

It is evident from Figure 2 that the $h/c = 8$ pitching moment results are in error. This error was even more marked when computations were attempted at larger h/c values. This problem is thought to be due to the computational grid used in TSFOIL. A constant number of grid points was used irrespective of the h/c value, and as h/c was increased the grid was linearly stretched

normal to the flow direction. For large h/c the grid becomes excessively sparse near the model and errors occur particularly near the leading edge velocity peak. The C_m results are a much more sensitive indicator of such errors than the C_L results.

In Figures 3 and 4 calculated pressure distributions for the NACA 0006 in a solid wall tunnel with $h/c = 3$ and 1, and in free air at nominal and corrected conditions are presented. In interpreting these pressure distributions it should be remembered that blockage interference effectively changes the C_p scale, lift interference produces a differential change in upper and lower surface C_p's near the leading edge and stream curvature alters the variation of the loading along the chord. To facilitate comparison between the tunnel and corrected condition free air results the tunnel pressure distributions have been corrected for blockage. Any blockage effects evident in Figures 3 and 4 are therefore due to additional blockage not predicted by linear interference theory. From Figures 3 and 4 it can be seen that similar general effects occur for correctable ($h/c = 3$) and uncorrectable ($h/c = 1$) conditions although they are greatly exaggerated in the latter case. The effect of stream curvature is clearly evident in both figures, the tunnel pressure distribution showing less loading forward and more loading aft than the free air pressure distribution at the corrected conditions. These differences in pressure distribution should be cancelled by the linear interference theory correction terms $\frac{\pi}{2}\cdot\frac{\delta_1}{\beta^2}\left(\frac{c}{h}\right)^2 C_L$ and $\frac{\pi}{8}\cdot\frac{\delta_1}{\beta^2}\cdot\left(\frac{c}{h}\right)^2 C_L$ being applied to C_L and C_m respectively. It is interesting to note that the solid tunnel walls have the greatest influence on the suction side pressure distribution and the application of corrections actually degrades the agreement between the lower surface tunnel and free air pressure distributions.

Linear interference theory is only strictly applicable to subcritical flows. However, experience[8] has shown that it can also give useful results when applied to slightly supercritical flows. In an attempt to establish some quantitative guideline to the limits of applicability of the linear theory a series of supercritical flows were computed. The C_L and C_m errors obtained from these calculations are presented in Figures 5 and 6. From these figures it can be seen that, unlike the subcritical results, no universal relationship between error and h/c is evident and the minimum acceptable h/c varies widely. In an effort to obtain some collapse of the scattered results shown in Figures 5 and 6 the variation of corrected C_L and C_m errors with a number of parameters was investigated. The most useful correlating parameter from a practical point of view which was discovered was y_{sonic}/h (where y_{sonic} = maximum height of supersonic region on aerofoil). The value of y_{sonic} in actual tunnel tests could be obtained from sidewall pressure measurements or optical flow visualisation. The plots of corrected C_L and C_m errors against y_{sonic}/h presented in Figure 7 show considerable scatter but nevertheless provide some quantitative guidance as to acceptable supersonic region size. From Figure 7 it appears that for accurate results with a high confidence level y_{sonic}/h should not exceed about 0·04. It should be noted that for very slightly supercritical conditions the subcritical limitation $h/c \geqslant 3{\cdot}0$ and not the limitation $y_{sonic}/h \leqslant 0{\cdot}04$ will govern the maximum model size.

A typical solid wall supercritical pressure distribution along with nominal and corrected condition free air results are plotted in Figure 8. To facilitate comparisons the solid wall distribution has been corrected for blockage. The most obvious effect of soild wall interference is the rearward shift of the upper surface shock wave. As for the subcritical results the lower surface pressure distribution is comparatively insensitive to solid wall interference.

3.2 Open Jet

Open jet wind tunnels were common in the early days of experimental aerodynamics but are now mainly used for non-lifting bluff body tests where their theoretical zero wake blockage characteristics[3] are attractive. However, since some lifting aerofoil tests are conducted in open jet tunnels they will be studied briefly here. The mathematical formulation of the open jet boundary conditions is straightforward and the predictions of linear interference theory would be expected to apply quite well in practice. It should be noted that the linear theory assumes equal pressures on the upper and lower jet boundaries while some tunnel arrangements cause a pressure difference to be set up when the jet is deflected by a lifting model.[3] Any such pressure difference would significantly reduce the accuracy of linear interference theory.

Preliminary calculations using the open jet option (BCTYPE = 3)[5] in TSFOIL showed that the downwash at the model location was not correctly represented. All open jet calculations were therefore carried out using the porous wall option (BCTYPE = 5) with the porosity P set at 10^5. This porosity gives pressure coefficients very close to zero along the jet boundaries.

In Figures 9 and 10 the lift and pitching moment coefficient errors for some subcritical and supercritical computations in an open jet are presented. Some indication of the relative performance of solid wall and open jet test sections can be obtained by comparing Figures 9 and 10 with Figures 1, 2, 5 and 6. It should be remembered that this comparison favours the open jet for supercritical cases, since as the test section height is reduced the corrected Mach number is reduced for an open jet and increased for a closed tunnel. The most obvious difference between the two tunnel types is that for tunnel heights in the commonly used range ($3 \leqslant h/c \leqslant 8$) the open jet gives considerably greater lift coefficient errors before and after correction. A detailed examination of the cases computed failed to reveal any example where an open jet gave superior results to a closed solid wall tunnel.

At higher angles of attack a further problem would arise in that the large jet deflections caused by the model would lead to a breakdown of the assumptions implicit in the linear interference theory. The magnitude of this jet deflection can be illustrated by considering the case of a NACA 0006 aerofoil with $\alpha = 2°$, $M = 0{\cdot}55$ and $h/c = 3$ in an open jet. The corrected model incidence is $1{\cdot}0677°$, the stream direction $4{\cdot}575c$ upstream from the model is $0°$ and $3{\cdot}875c$ dowstream from the model it is $-1{\cdot}445°$. It can be seen that for this quite practical h/c value the jet deflection is considerably greater than the flow incidence experienced by the model.

Subcritical and supercritical pressure distributions for an open jet with free air distributions for comparison are plotted in Figures 11 and 12. As for all previous pressure distributions the open jet curves have been corrected for blockage. The effect of the large incidence correction is illustrated by the considerable difference between the nominal condition free air and corrected condition free air results. The open jet results clearly show the effect of stream curvature of the opposite sign to that experienced in a solid wall tunnel. It is interesting to note that in contrast to a solid wall tunnel (Fig. 8) the open jet does not produce an upper surface shock displacement from the corrected free air location (Fig. 12).

3.3 Porous Wall

Since the 1950s perforated walls, which are usually considered to present a homogeneous porous boundary, have been widely used in transonic wind tunnels. They are particularly valuable at low supersonic speeds where it is desired to prevent the reflection of incident shock waves. There is some indication that the homogeneous porous wall boundary condition $\delta_p = \rho U w_n / P$ (where δ_p = pressure drop across wall and w_n = velocity normal to wall) used in linear interference theory is not a particularly accurate model of the real perforated wall boundary condition. There is evidence to suggest that the effective local porosity of the wall depends on the local Mach number and whether the flow is into or out of the test section. Despite this uncertainty linear interference theory is applied to perforated wall tunnels with some success.

Linear theory indicates that with a suitable selection of P it is possible to achieve zero downwash or zero stream curvature or zero blockage. Unfortunately these three desirable conditions occur for different values of P and can not be achieved simultaneously. It was hoped that flow computations for each conditions would indicate which was the most desirable to aim for in practice. The condition of zero downwash occurs for $P = 0$ which is identical to the solid wall boundary considered in Section 3.1. Zero stream curvature is predicted when $\beta/P = 0{\cdot}78$ and zero blockage when $\beta/P = 1{\cdot}278$. It should be noted that the porosity appears in the form β/P in the interference theory so P has to be changed with the tunnel Mach number if a given interference condition is to be maintained.

Unfortunately for values of P leading to zero stream curvature or zero blockage TSFOIL showed a marked disinclination to converge while for higher or lower values of P it converged readily. Eventually by altering the pseudo-time coefficient EPS three converged cases were obtained for subcritical zero stream curvature flow. It was not found possible to compute any supercritical or zero blockage cases.

The lift and pitching moment errors for the three converged cases are plotted in Figure 13. Comparing these results with the earlier solid wall (Figs 1 and 2) and open jet (Figs.. 9 and 10)

results it can be seen that the corrected lift coefficient errors for the porous walls lie between those for the two earlier wall types. The corrected pitching moment coefficient errors for the porous wall are greater than those obtained for the earlier wall types. An example of porous wall and comparative free air pressure distributions is presented in Figure 14.

3.4 Slotted Walls

Slotted walls have been widely used in transonic wind tunnels since the original development of these facilities in the early 1950s. They give inferior incident shock cancellation to perforated walls at supersonic speeds but are generally considered to be preferable from an interference point of view at subsonic speeds. In linear interference theory slotted walls are characterised by a geometric parameter F and the cross flow resistance or porosity P. This general slotted wall boundary condition is not incorporated in TSFOIL and only the inviscid $P = \infty$ condition is available. Despite this limitation it was considered that a theoretical investigation of slotted wall interference would provide a valuable guide for real tunnel wall design.

As for the porous wall discussed previously, linear theory indicates that zero downwash, zero stream curvature and zero solid blockage can be achieved in slotted tunnels for various values of F. Zero downwash occurs for $F = \infty$ which corresponds to the solid wall considered in Section 3.1. To determine which of the two remaining slotted wall conditions was most favourable, comparative computations were carried out on a subcritical and a supercritical test case for $F = 1 \cdot 59$ (zero stream curvature) and $F = 1 \cdot 1844$ (zero solid blockage). The results of this comparison are plotted in Figures 15 and 16. From these two figures it is evident that before correction the zero stream curvature results show lower errors than the zero solid blockage results and after correction the positions are reversed. On the basis of this result the zero blockage ($F = 1 \cdot 1844$) wall type was considered to be superior and was investigated in more detail.

In Figures 17 and 18 the lift and pitching moment errors for a range of subcritical and supercritical test cases with $F = 1 \cdot 1844$ are plotted. From these two figures it appears that this wall condition is better than any of those considered previously in this Note. For subcritical flow near zero corrected C_L and C_m errors are obtained for $h/c \geqslant 2$. All the supercritical flows showed acceptable corrected C_L errors for $h/c \geqslant 3$. Two highly supercritical test cases (with supersonic region height/chord ratios of 0·55 and 1·35 for the NACA 0006, $\alpha = 3°$, $M = 0 \cdot 75$ and the NACA 0012, $\alpha = 2°$, $M = 0 \cdot 78$ respectively) required a minimum h/c ratio of 4 for reasonably small corrected C_m errors (Fig. 18). The correlation factor (sonic region height/tunnel height) used with the solid wall results also produces some collapse of the scattered errors apparent in Figures 17 and 18. The results of this correlation are presented in Figure 19. A comparison between Figures 7 and 19 clearly shows the advantage of the $F = 1 \cdot 1844$ slotted walls over the solid walls for supercritical tests. To obtain a C_L error after correction of less than $1 \cdot 5\%$ the value of y_{sonic}/h for the slotted walls must be less than 0·2 whereas for a solid wall tunnel y_{sonic}/h must be less than about 0·06 for the same error.

Two slotted wall pressure distributions with comparative free air results are plotted in Figures 20 and 21. These two figures show that despite the small h/c values, the tunnel and corrected condition free air results are very similar. None of the three types of interference (downwash, stream curvature or blockage) appear to dominate and the supercritical case does not show a significant shock displacement.

Taken overall the zero blockage ideal (inviscid) slotted wall appears most attractive for subsonic and transonic ($M < 1$) aerofoil tests. It would seem well worthwhile to investigate methods of reducing viscous effects for slotted walls to see how closely the excellent theoretical performance could be approached in practice.

4. CONCLUSION

The solid wall investigation showed that, for subcritical test conditions, linear interference theory gave very accurate results for $h/c \geqslant 3$. For supercritical tests linear theory proved less successful and the supersonic region height/h ratio had to be less than about 0·04 if results of high accuracy were required. Solid tunnel walls are not really suitable for supercritical or near critical aerofoil tests since, due to the solid blockage interference, the model supersonic region can rapidly grow to an excessive size as the Mach number of incidence is increased.

The open jet investigation revealed very much greater corrected lift errors than those found with solid walls. Interference theory appeared to work better at higher Mach numbers than low ones but this is regarded as purely fortuitous and not as a good reason for using an open jet tunnel for high transonic tests. It is suggested that the use of an open jet test section would only be justified for bluff body tests where a very large wake was expected. Under these conditions the theoretically zero wake blockage of an open jet could be an advantage.

The investigation of porous walls was severely limited by convergence problems with TSFOIL. Insufficient cases were successfully computed to reach any positive conclusions. However, the results obtained suggest that the interference in a porous tunnel is part way between that of a solid wall and open jet. It is tentatively suggested that porous walls should only be used where shock wave cancellation is important.

A preliminary investigation into ideal slotted walls indicated that the zero blockage wall configuration ($F = 1 \cdot 1844$) gave smaller corrected lift and pitching moment errors than the zero stream curvature wall ($F = 1 \cdot 59$). Further investigations of the zero blockage wall showed that linear interference theory gave good results for $h/c \geqslant 2$ and supersonic region height/h ratios less than about $0 \cdot 2$. The above observations indicate that model sizes somewhat larger than customary may be possible in slotted wall tunnels.

An investigation of real slotted tunnel walls would be valuable to find how nearly the ideal (inviscid) predictions discussed here can be realised in practice. If real slotted walls with cross flow resistance were found (as appears probable) to have significantly inferior characteristics to ideal slotted walls, it would be worthwhile investigating methods of reducing slot viscous effects. It is tentatively suggested that some form of boundary layer control in the slots may be effective.

REFERENCES

1. Marschner, B. W., Young, R. L., and Broome, L. E.: Summer Faculty Systems Design Program. Integrating Wind Tunnels and Computers. AFOSR-77-3289, August 1977.

2. Numerical Methods and Wind Tunnel Testing. AGARD-CP-210, October 1976.

3. Garner, H. C., Rogers, E. W. E., Acum, W. E. A., and Maskell, E. C.: Subsonic Wind Tunnel Wall Corrections. AGARDograph 109, October 1966.

4. Murman, E. M., Bailey, F. R., and Johnson, M. L.: TSFOIL—A Computer Code for Two-Dimensional Transonic Calculations, Including Wind-Tunnel Wall Effects and Wave-Drag Evaluation. Aerodynamic Analyses Requiring Advanced Computers. Part II. NASA SP-347, 1975.

5. Stahara, S. S.: Operational Manual for Two-dimensional Transonic Code TSFOIL. NASA C.R. 3064, 1978.

6. Bauer, F., Garabedian, P., and Korn, D.: A Theory of Supercritical Wing Sections, with Computer Programs and Examples. Lecture Notes in Economics and Math. Systems 66. Springer-Verlag, 1972.

7. Catherall, D.: On the Evaluation of Wall Interference in Two-dimensional Ventilated Wind Tunnels by Subsonic Linear Theory. A.R.C. R. & M. 3819, 1978.

8. Lift-interference and Blockage Corrections for Two-dimensional Subsonic Flow in Ventilated and Closed Wind-tunnels. E.S.D.U. Data Item 76028, November 1976.

9. Wright, R. H.: The Effectiveness of the Transonic Wind-tunnel as a Device for Minimizing Tunnel-Boundary Interference for Model Tests at Transonic Speeds. AGARD Report 294, March 1959.

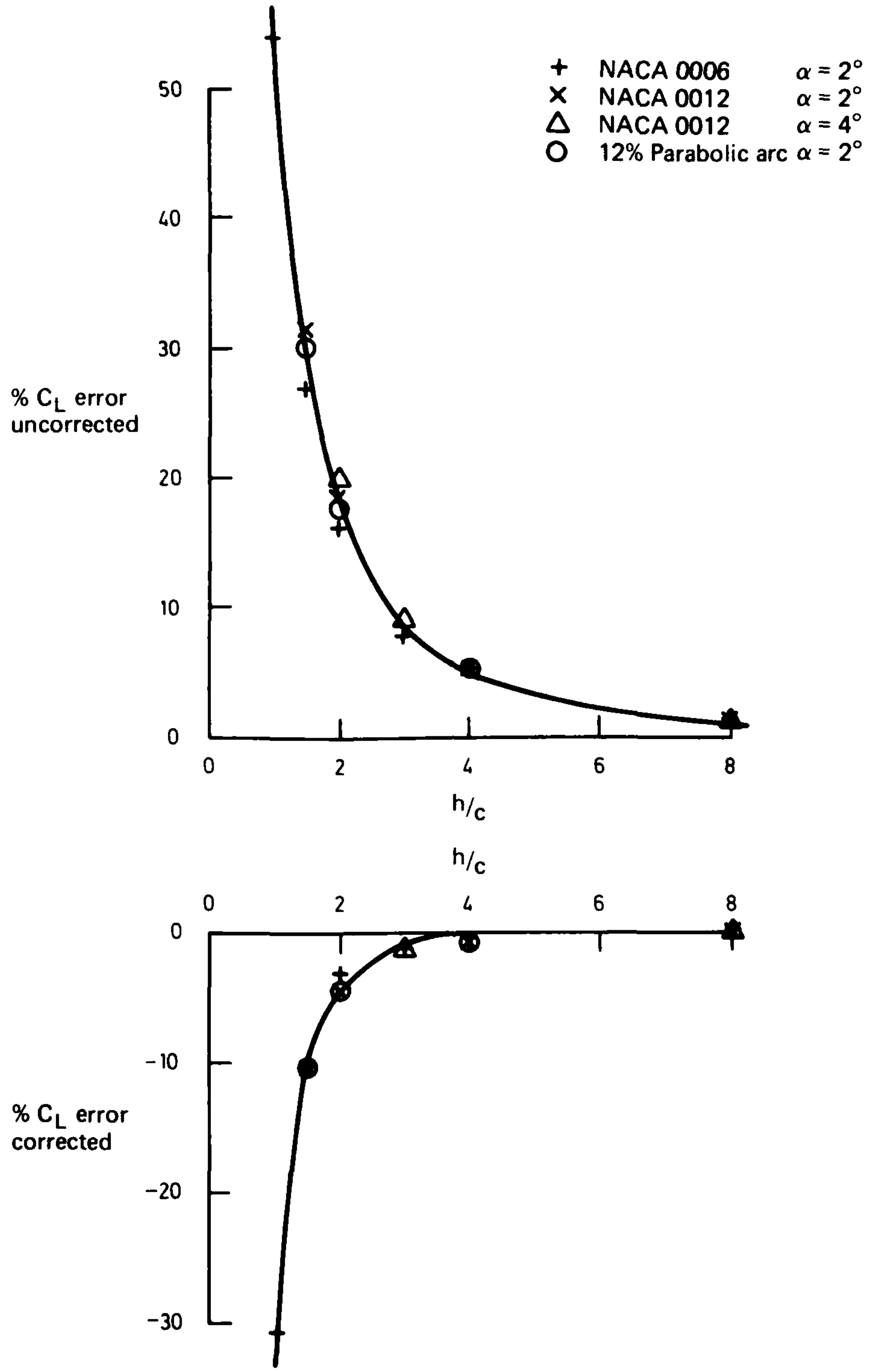

FIG. 1 LIFT COEFFICIENT ERROR, SOLID WALL, M = 0.55

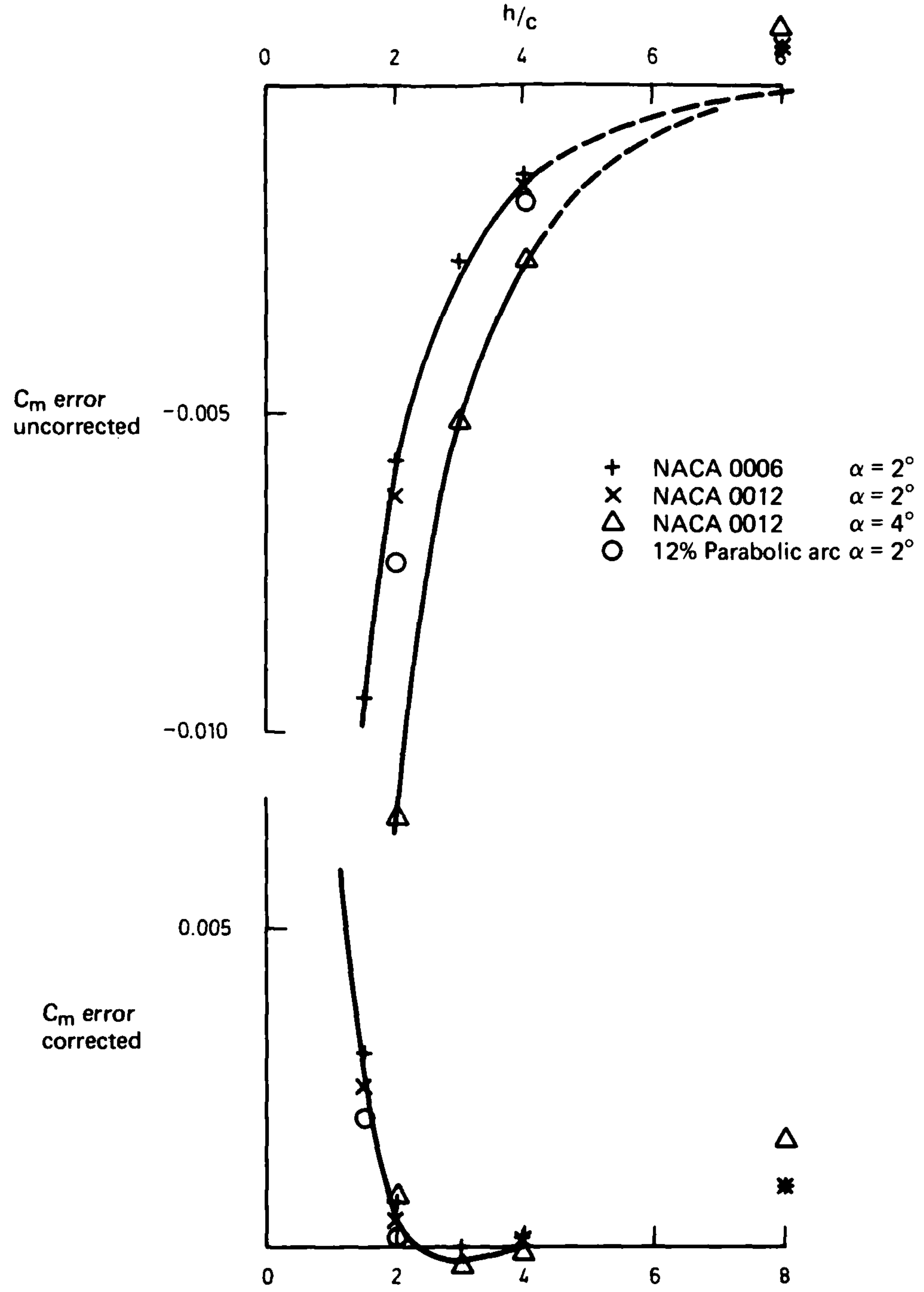

FIG. 2 PITCHING MOMENT COEFFICIENT ERROR, SOLID WALL, M = 0.55

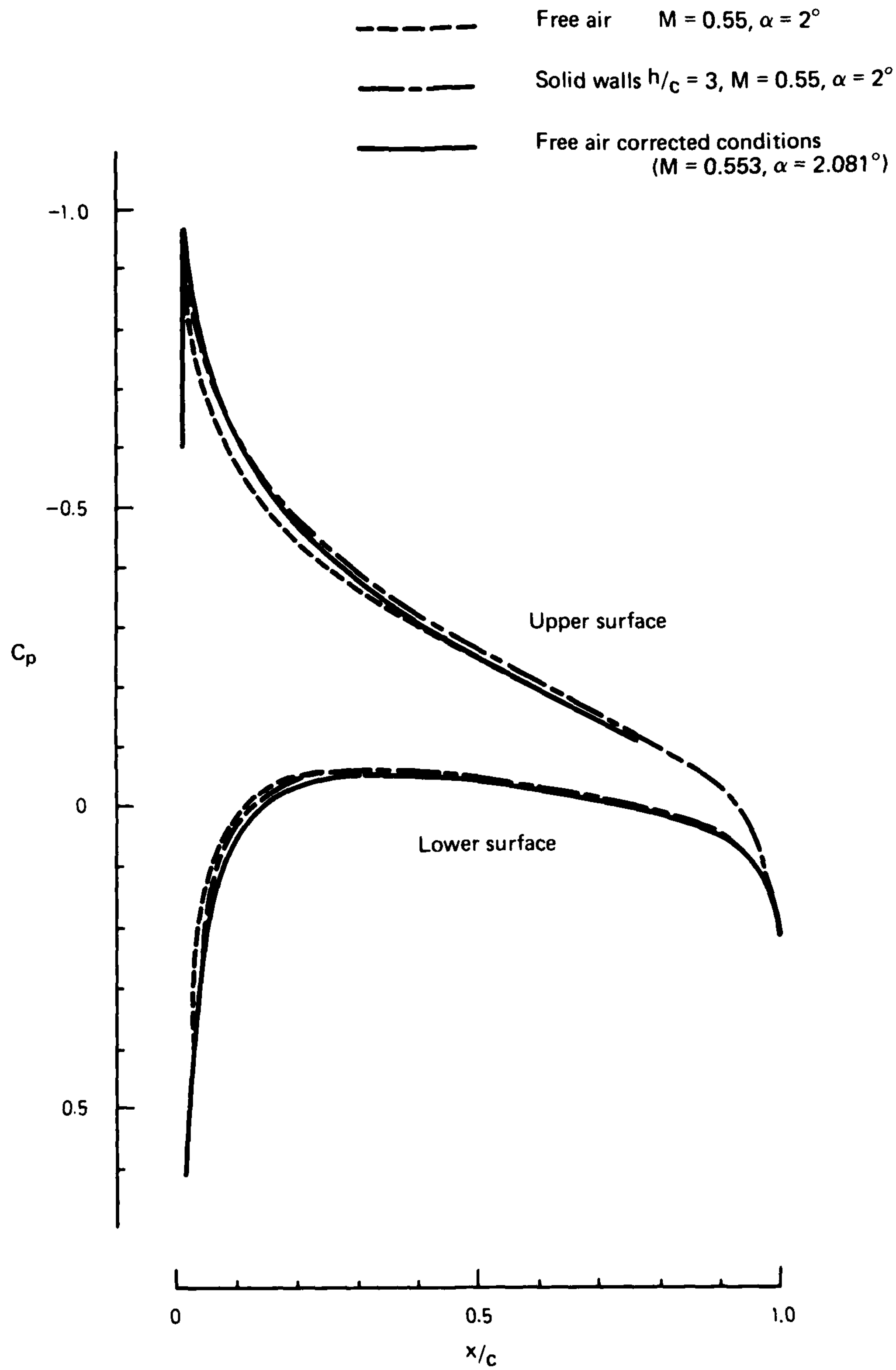

FIG. 3 PRESSURE DISTRIBUTIONS – NACA 0006 SOLID WALLS AND FREE AIR

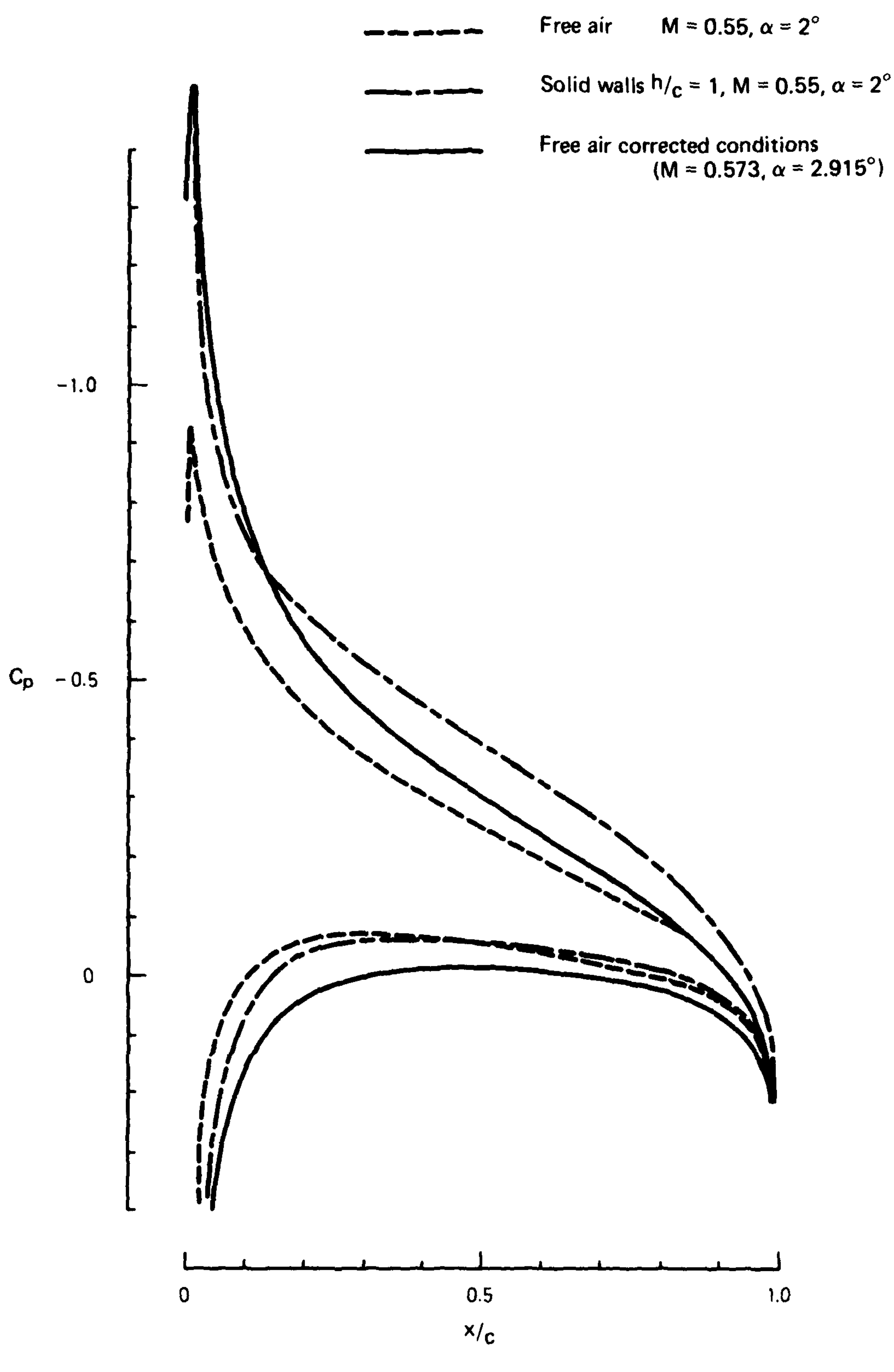

FIG. 4 PRESSURE DISTRIBUTIONS – NACA 0006 SOLID WALLS AND FREE AIR

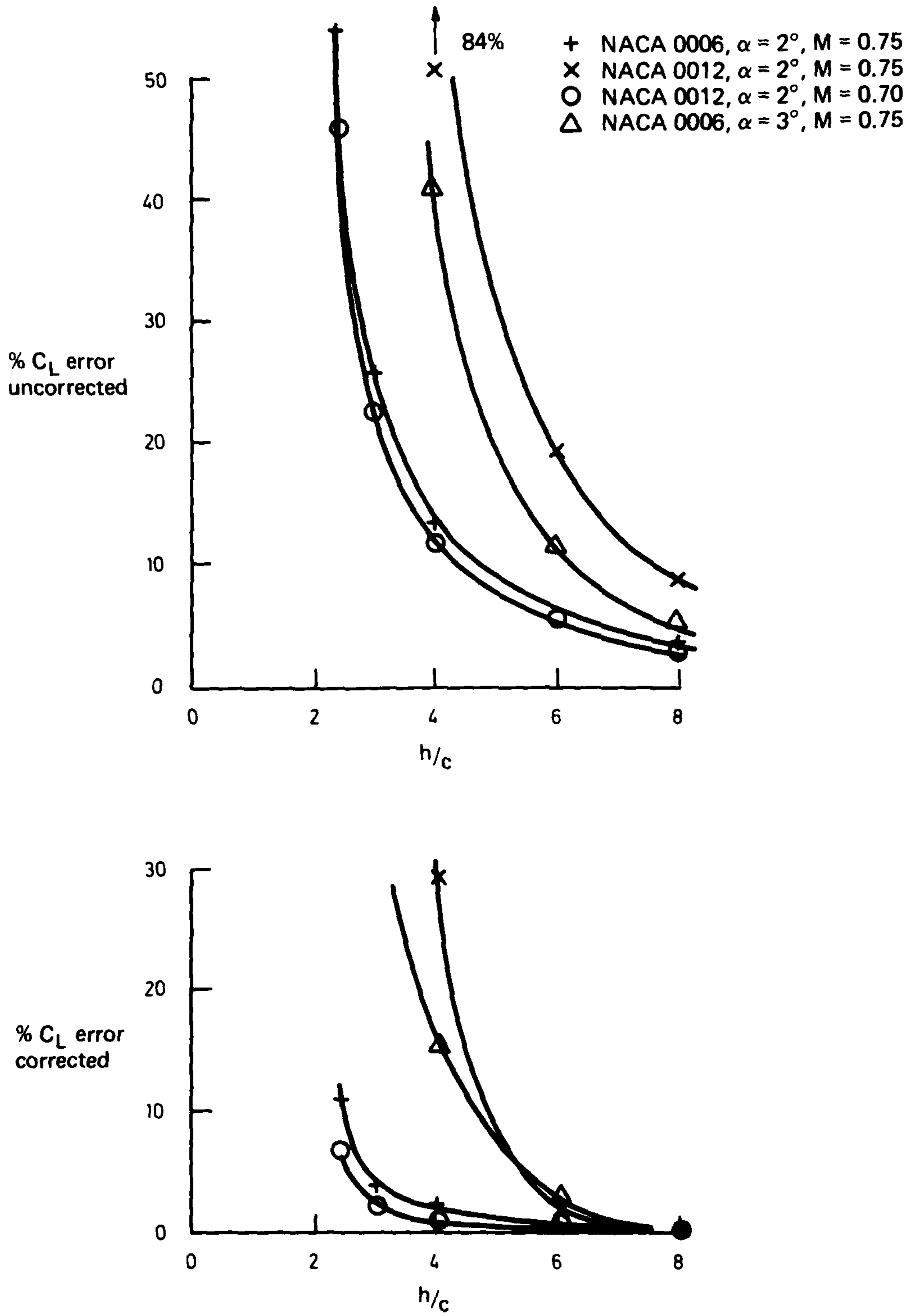

FIG. 5 LIFT COEFFICIENT ERROR, SOLID WALL, SUPERCRITICAL M.

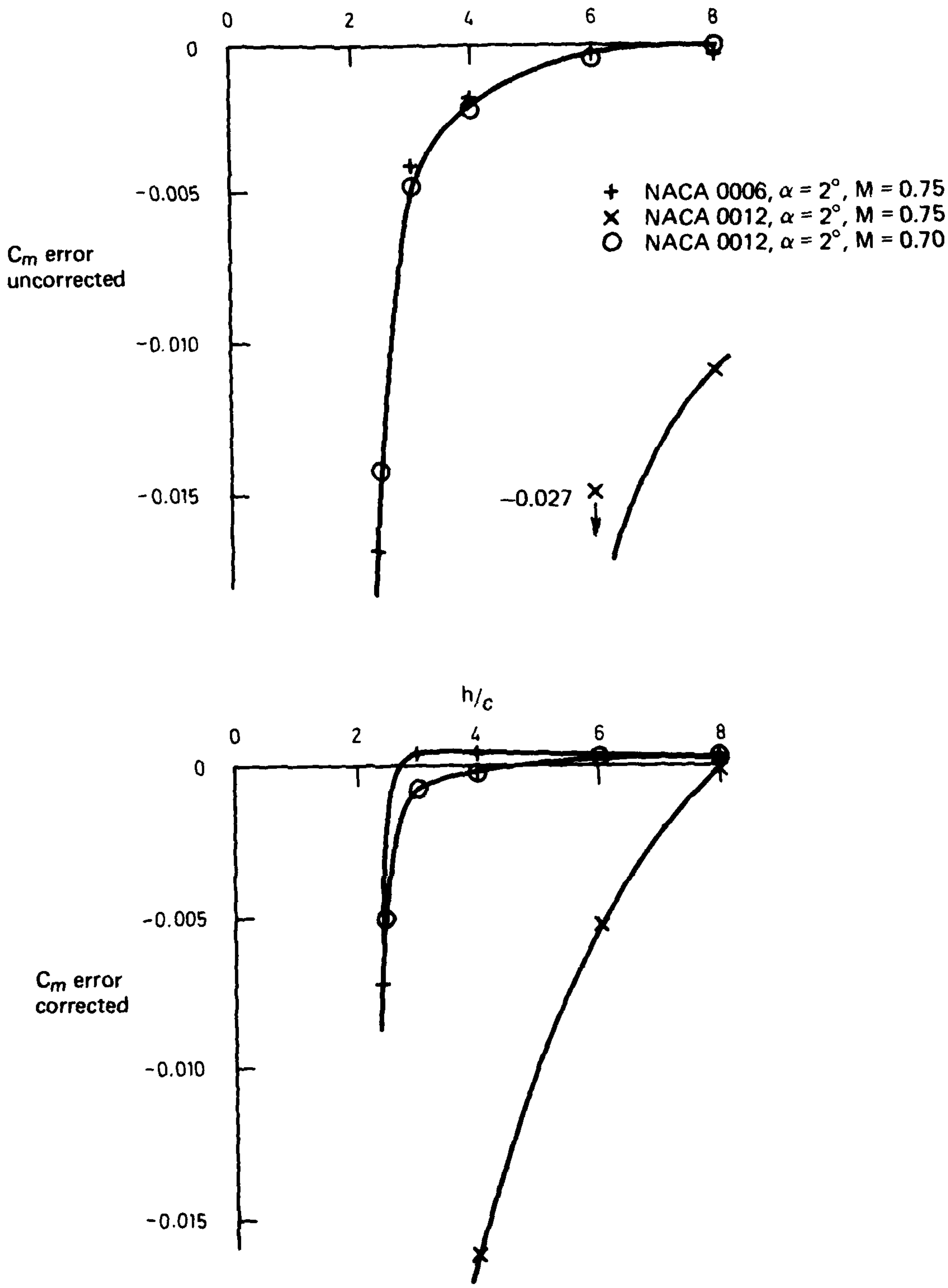

FIG. 6 PITCHING MOMENT COEFFICIENT ERROR, SOLID WALL, SUPERCRITICAL M

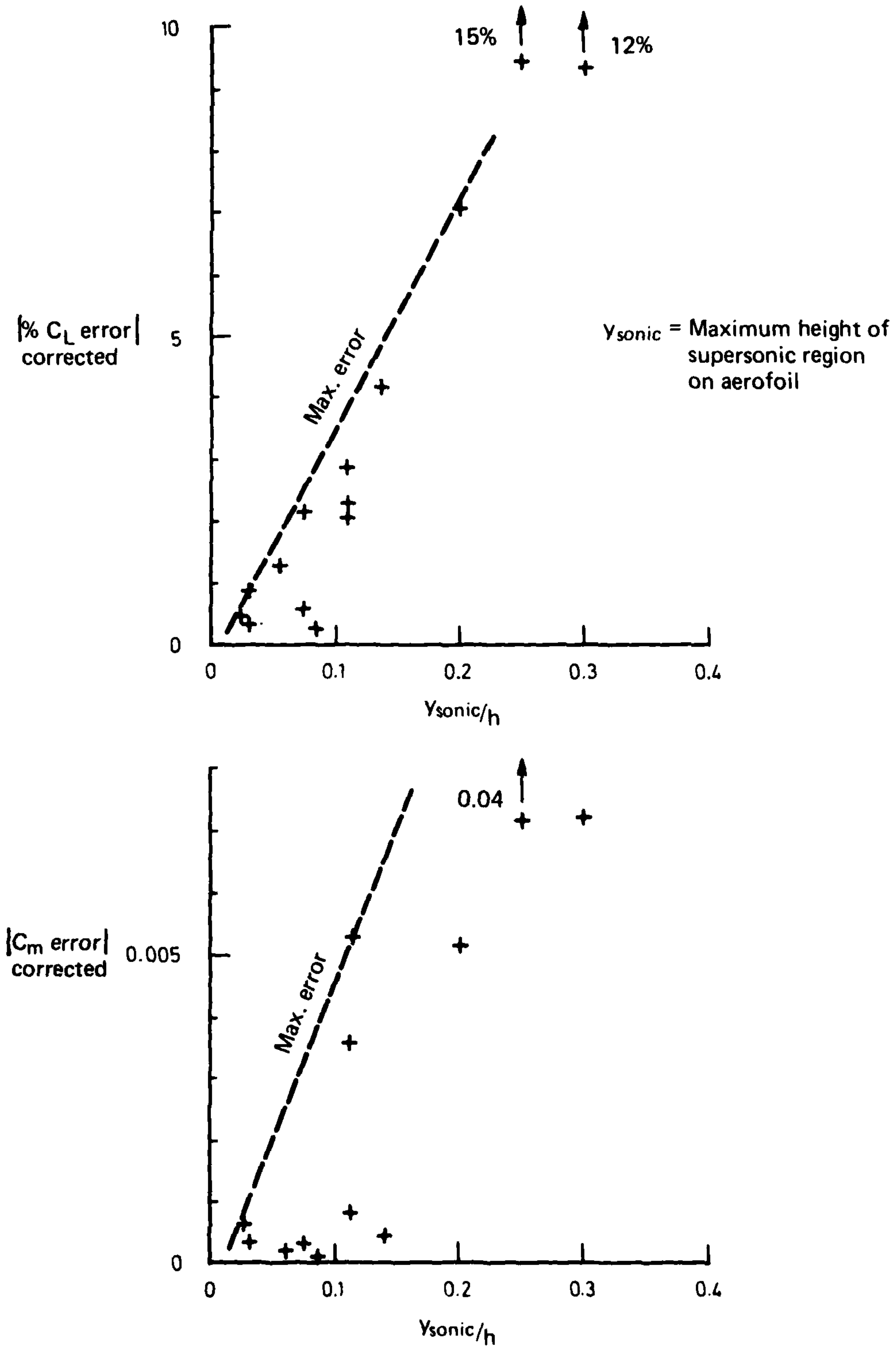

FIG. 7 CORRELATION OF SUPERCRITICAL SOLID WALL INTERFERENCE

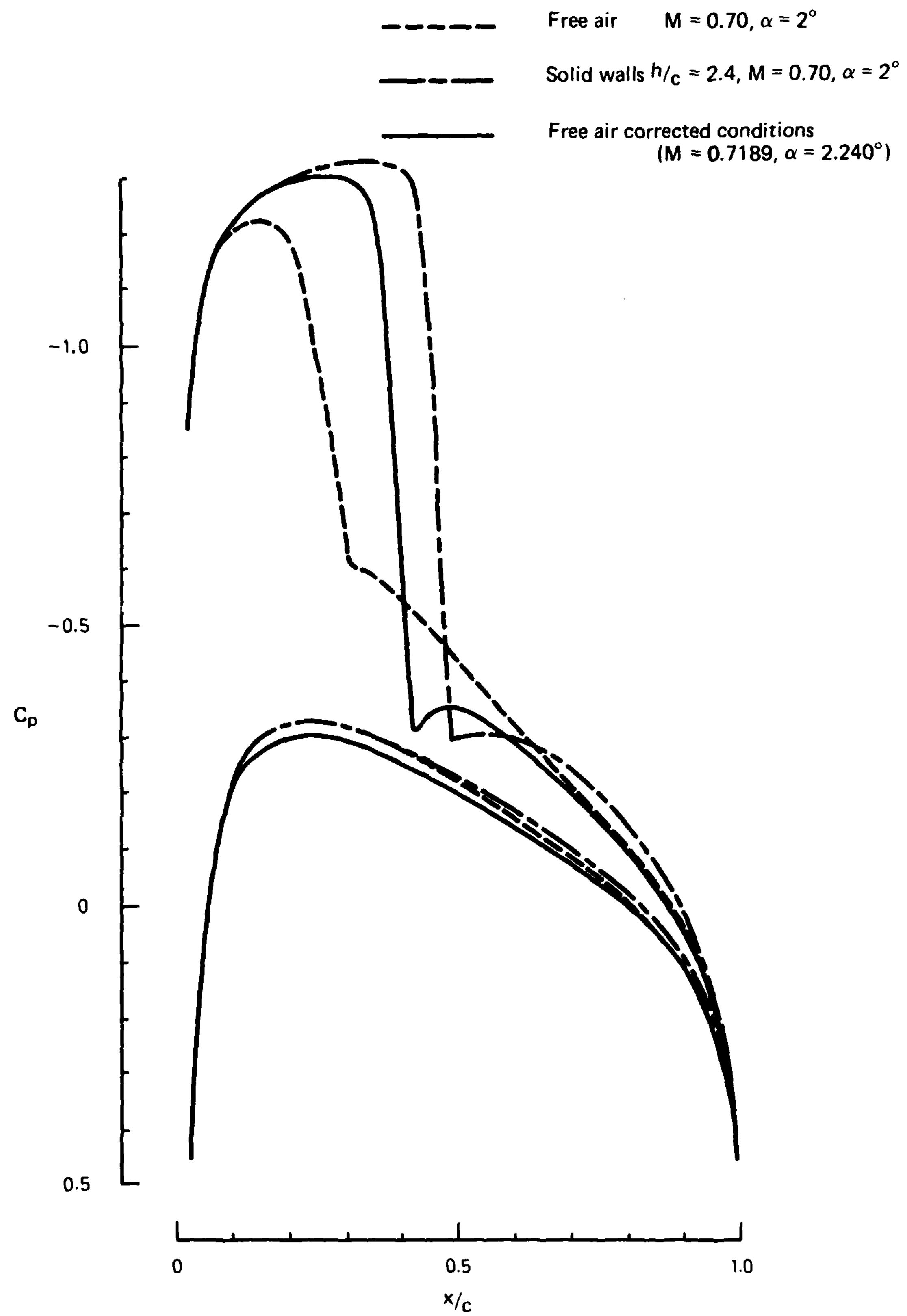

FIG. 8 PRESSURE DISTRIBUTIONS – NACA 0012 SOLID WALLS AND FREE AIR

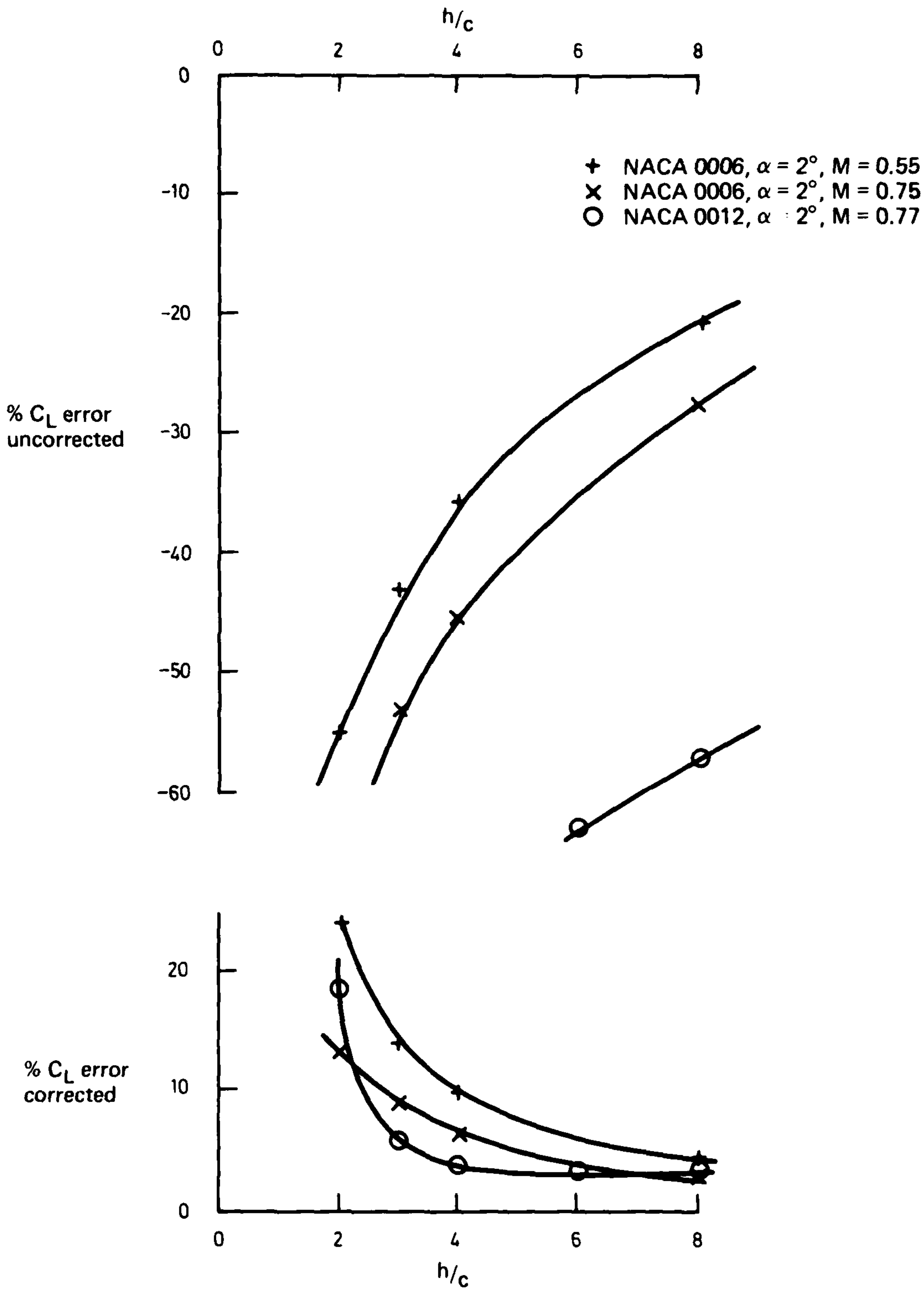

FIG. 9 LIFT COEFFICIENT ERROR, OPEN JET

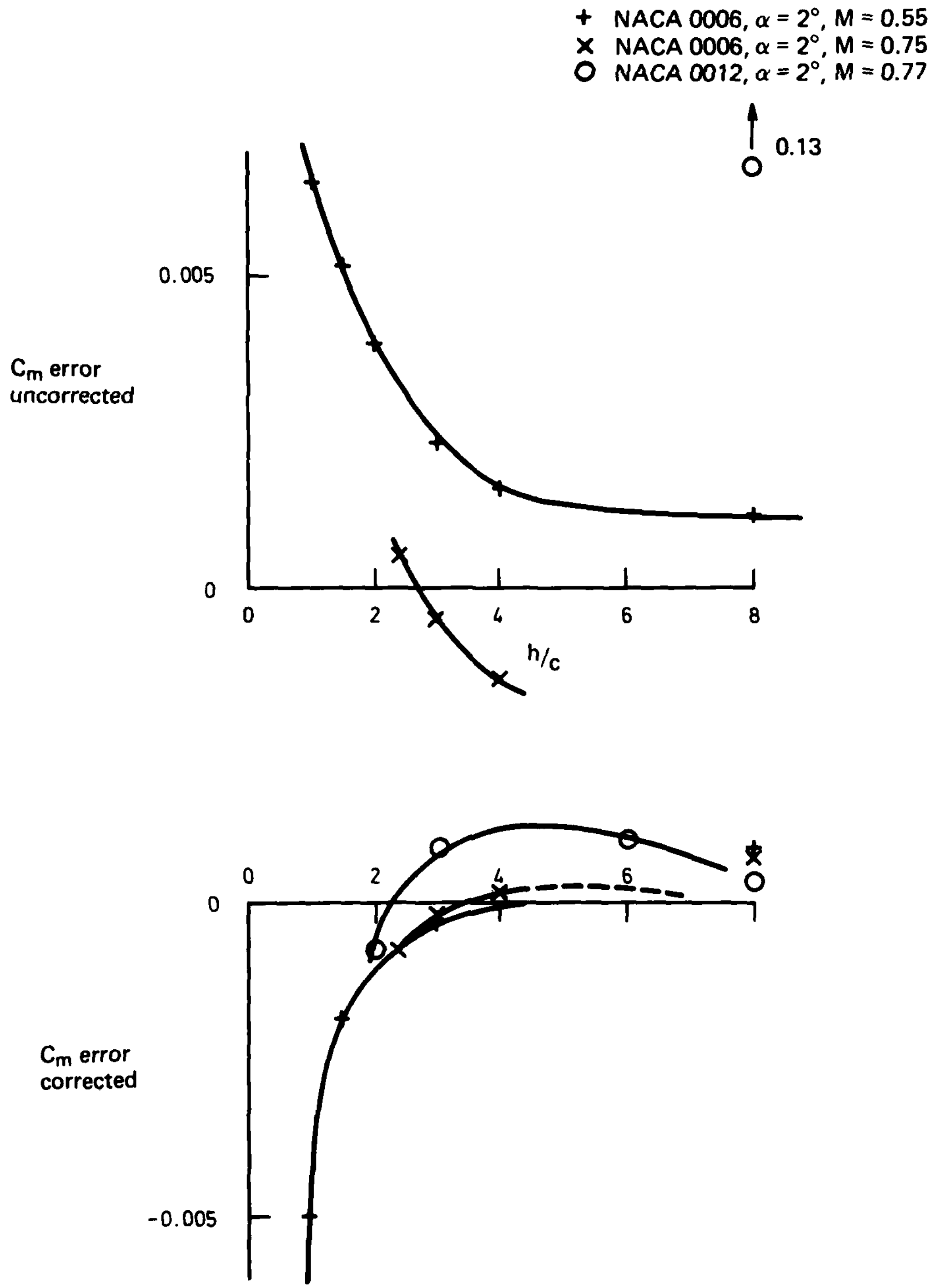

FIG. 10 PITCHING MOMENT COEFFICIENT ERROR, OPEN JET

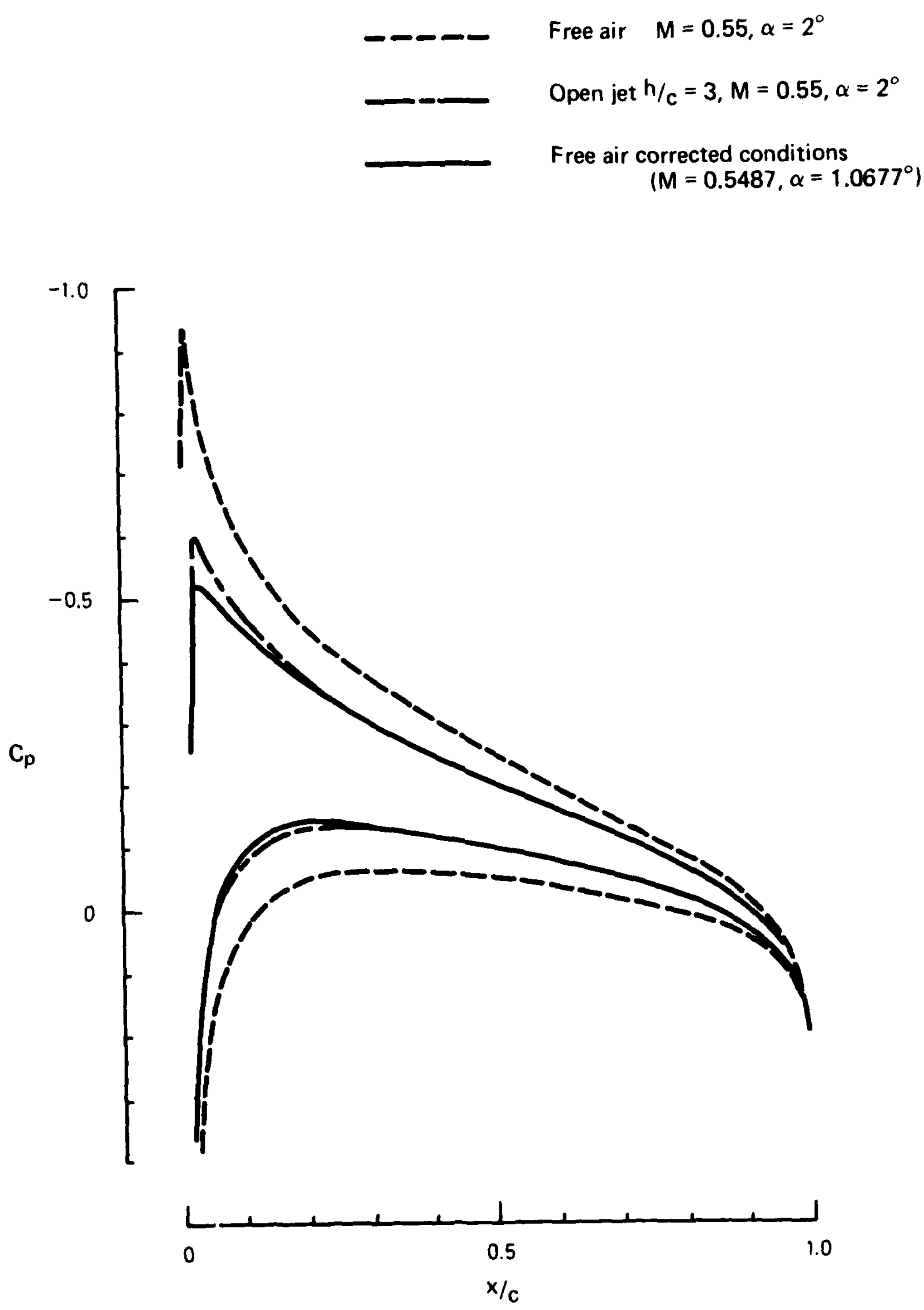

FIG. 11 PRESSURE DISTRIBUTIONS – NACA 0006 OPEN JET AND FREE AIR

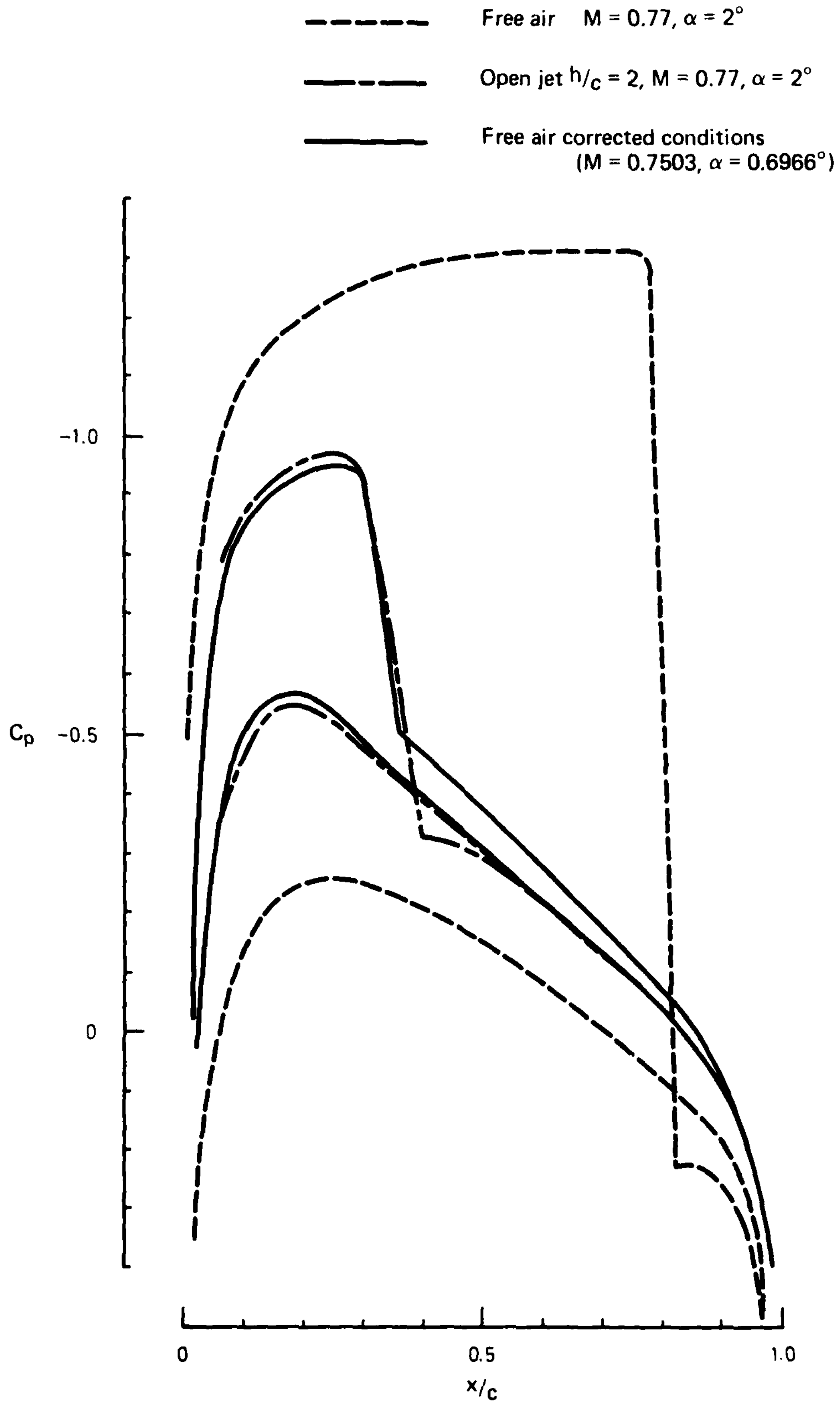

FIG. 12 PRESSURE DISTRIBUTIONS – NACA 0006 OPEN JET AND FREE AIR

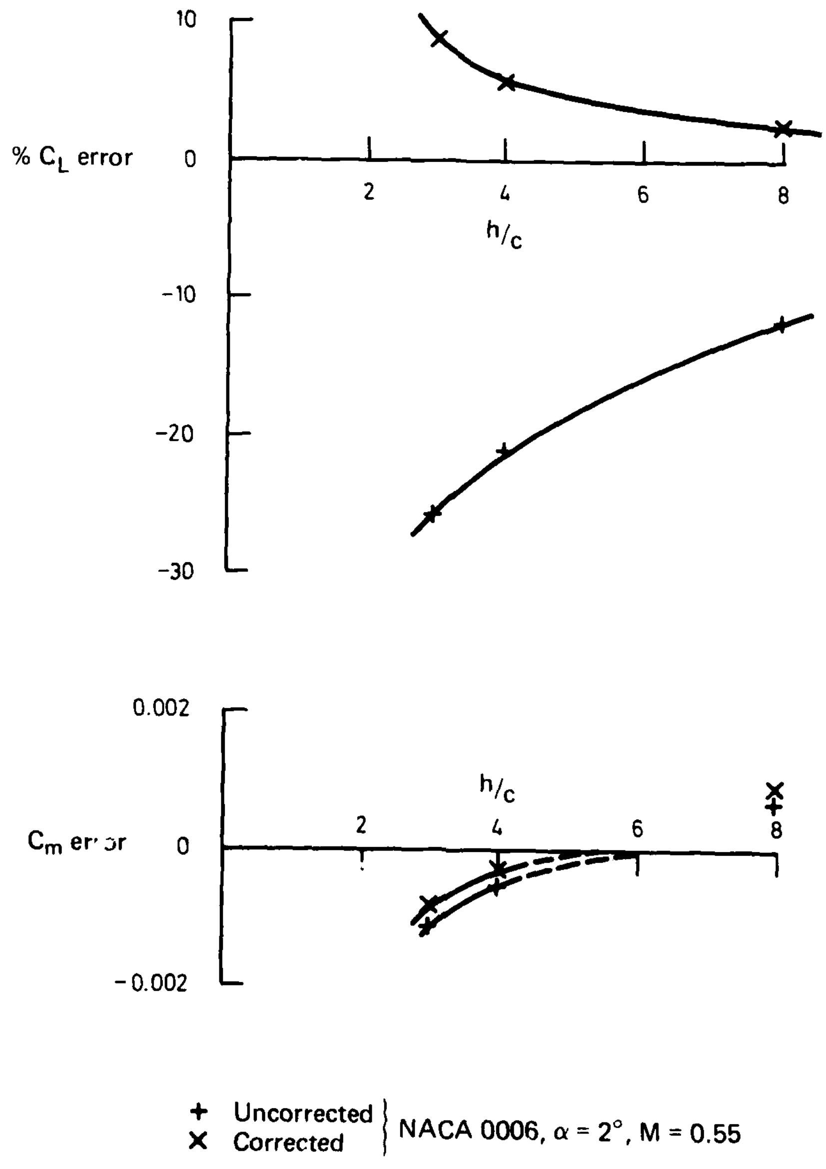

FIG. 13 LIFT AND PITCHING MOMENT COEFFICIENT ERRORS, POROUS WALL $\beta/_p = 0.78$

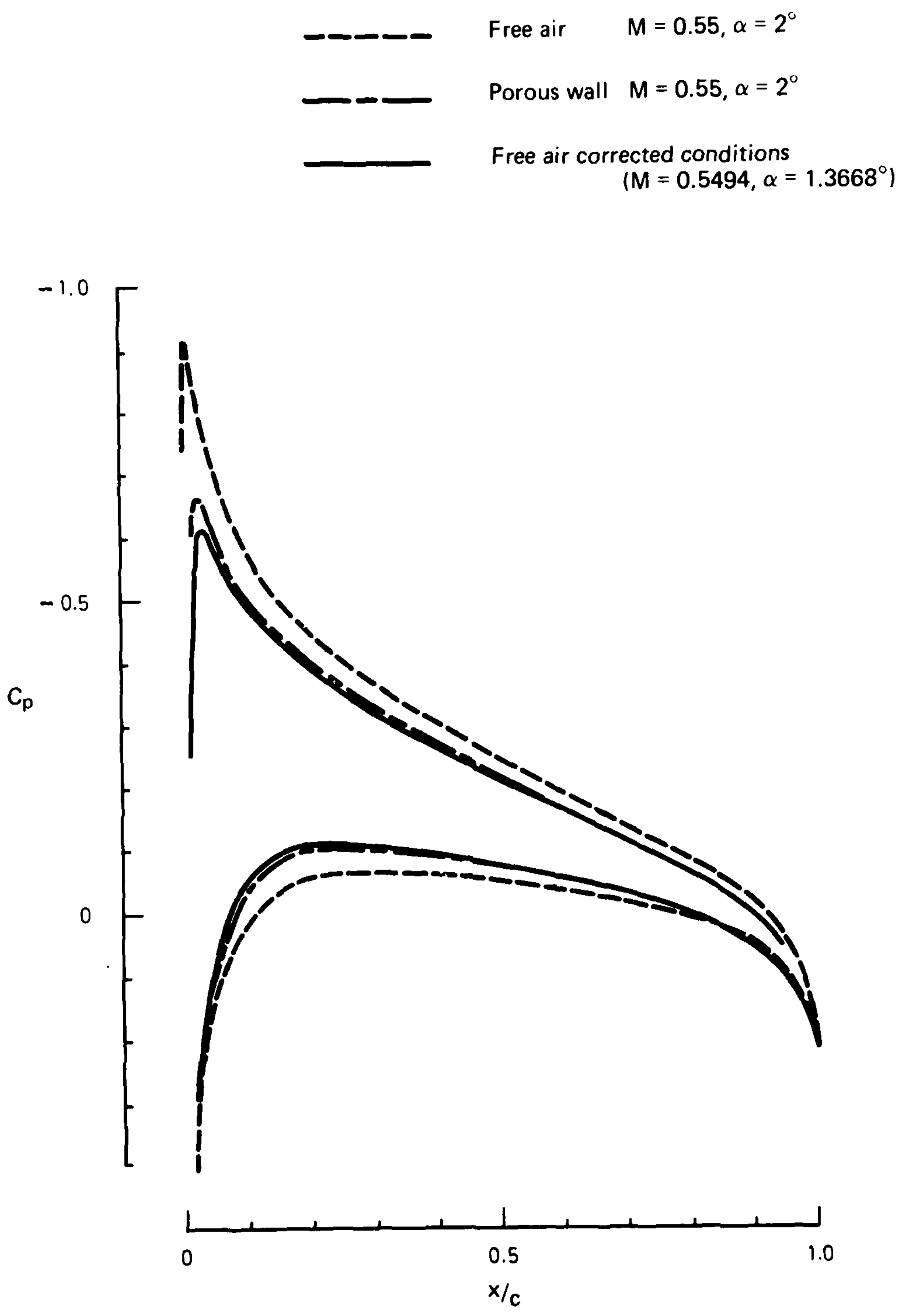

FIG. 14 PRESSURE DISTRIBUTIONS – NACA 0006
POROUS WALL ($\beta/_p$ = 0.78) AND FREE AIR

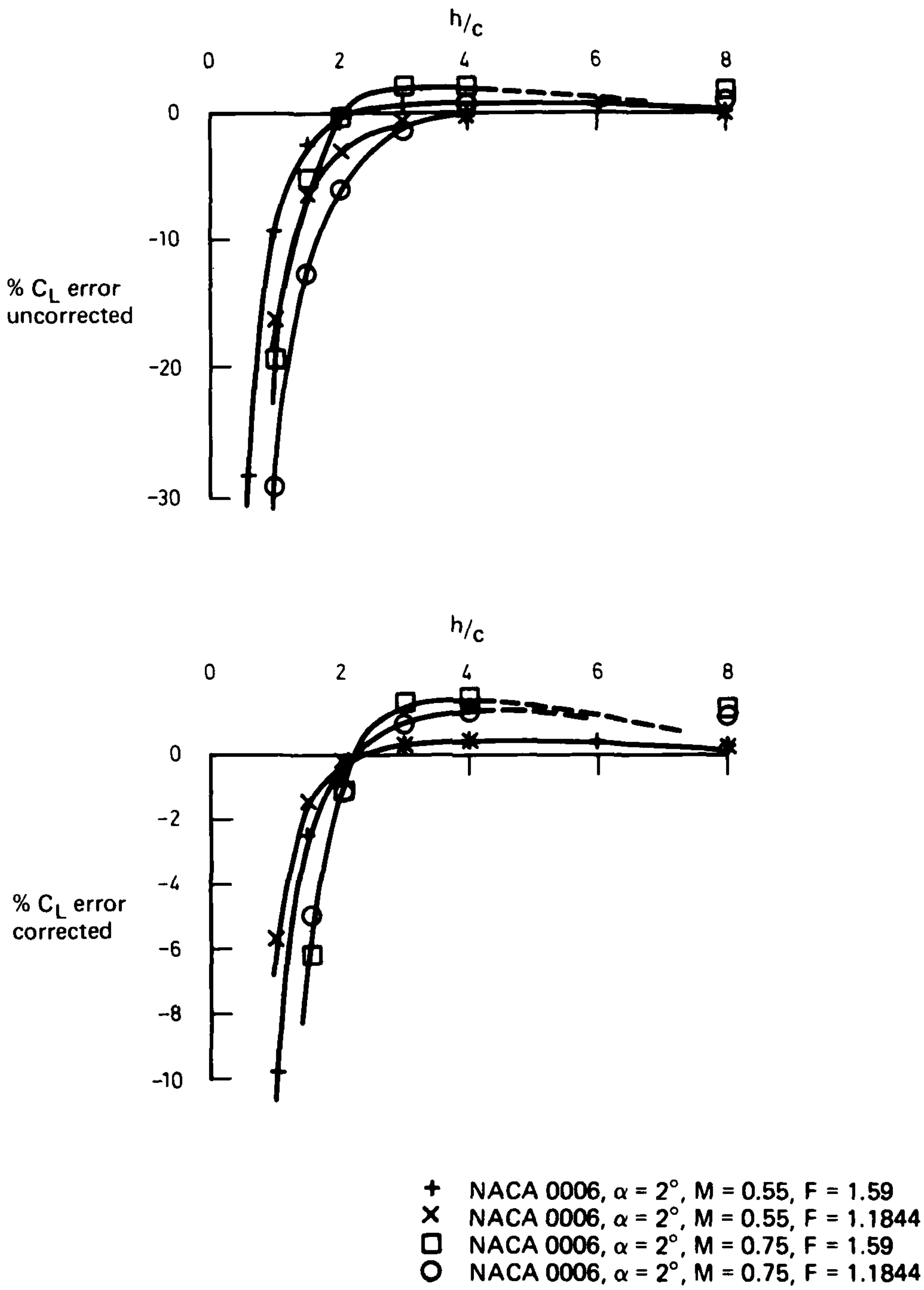

FIG. 15 LIFT COEFFICIENT ERROR, SLOTTED WALL
F = 1.59 AND F = 1.1844

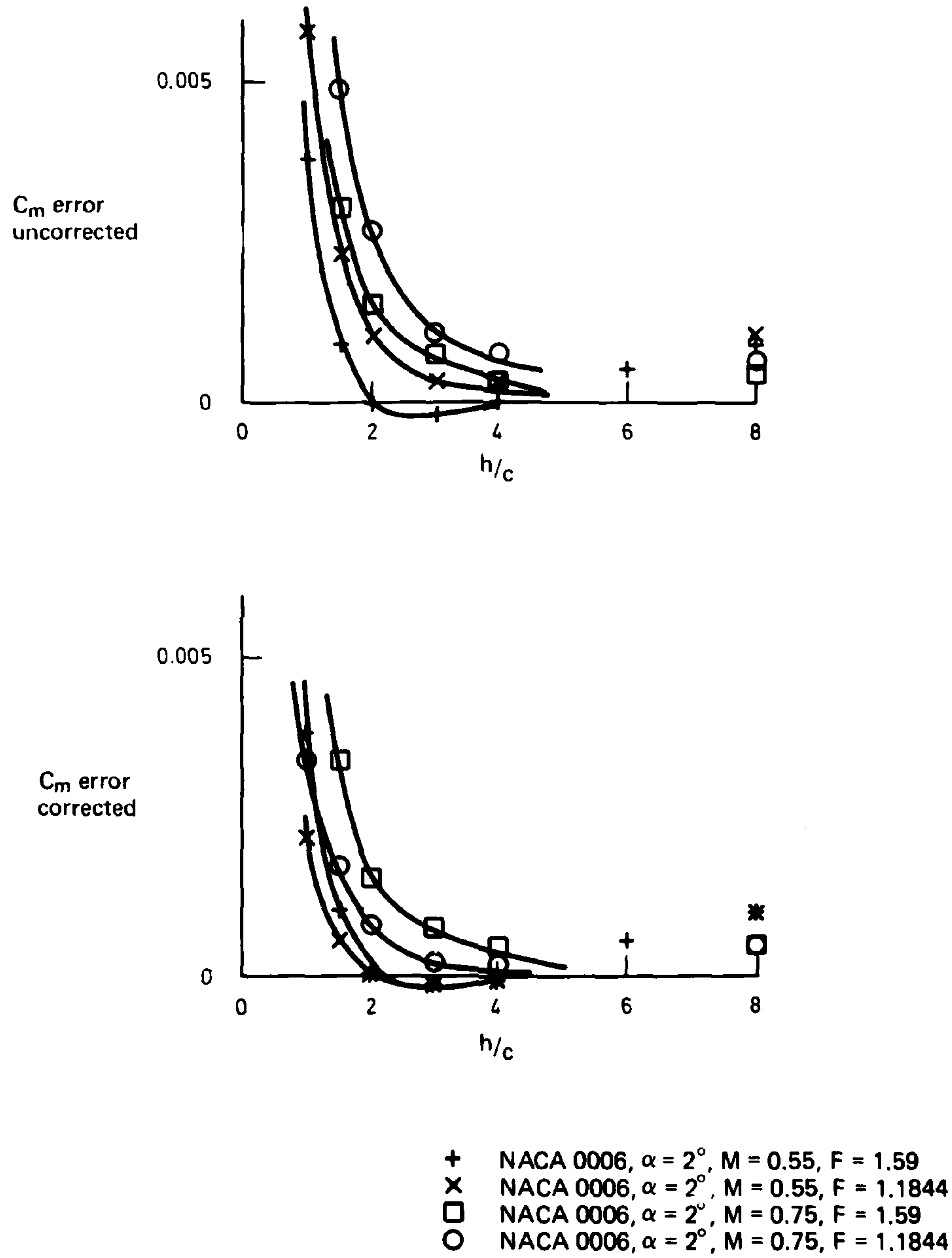

FIG. 16 PITCHING MOMENT COEFFICIENT ERROR, SLOTTED WALL
F = 1.59 AND F = 1.1844

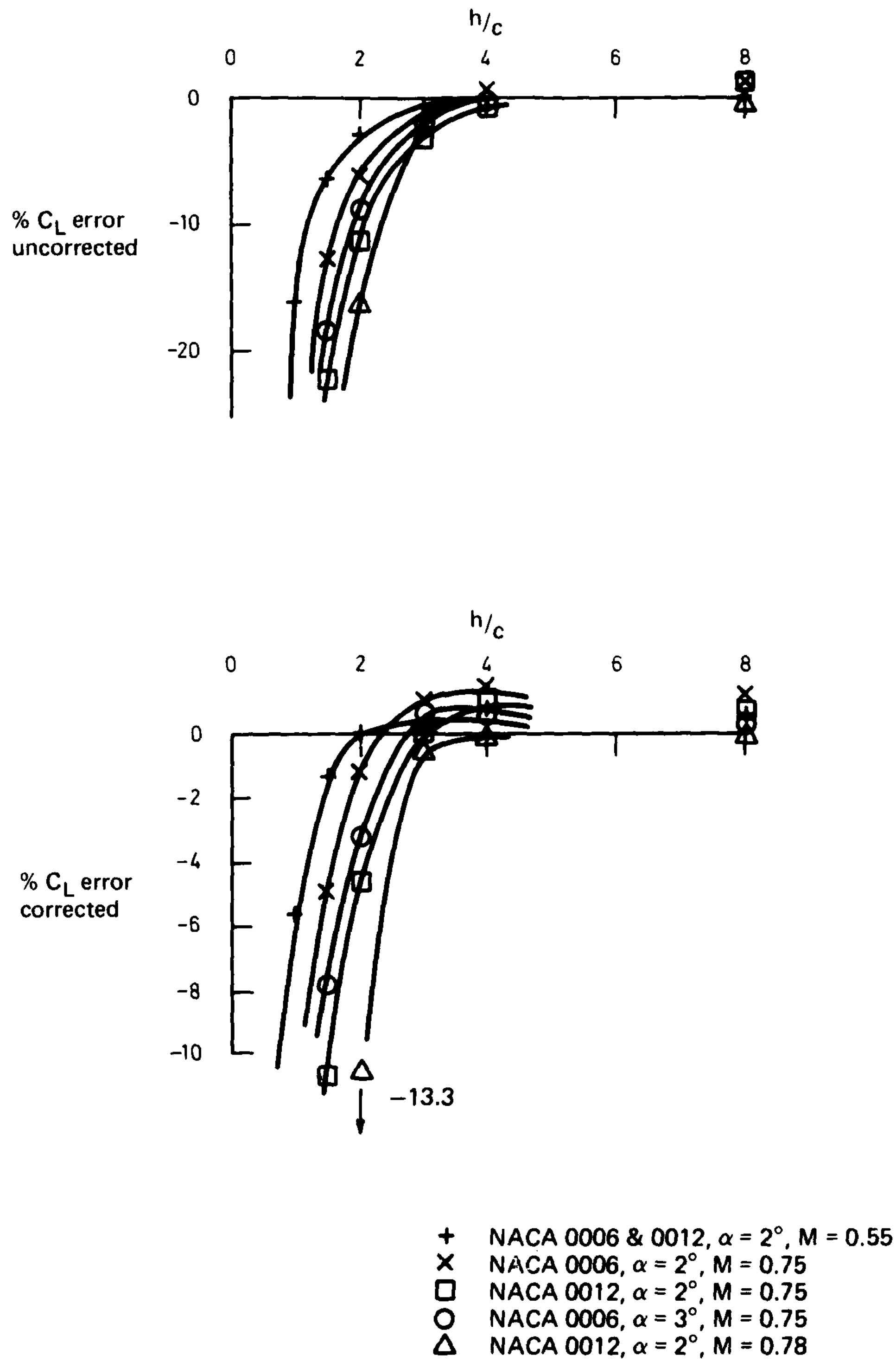

FIG. 17 LIFT COEFFICIENT ERROR, SLOTTED WALL F = 1.1844

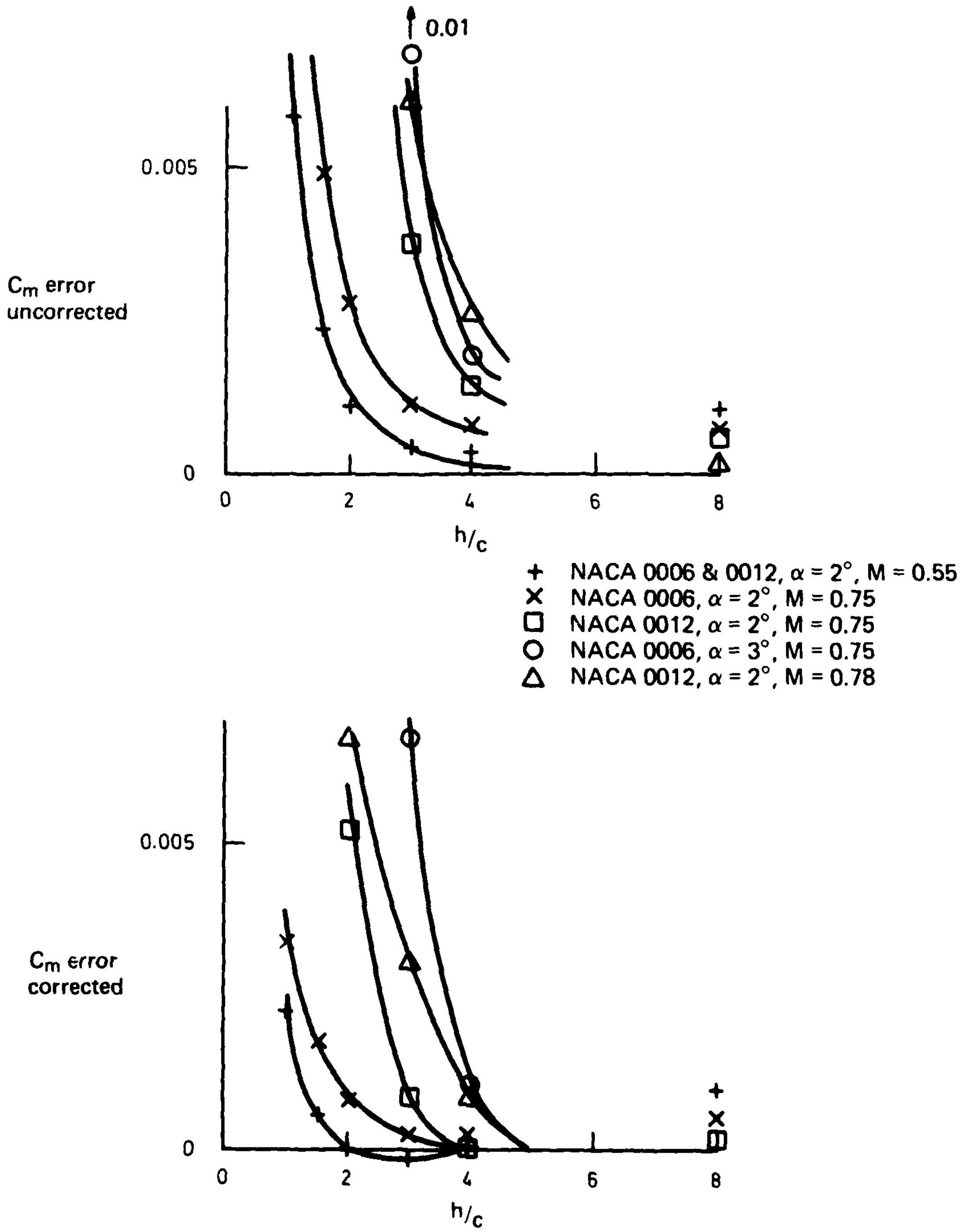

FIG. 18 PITCHING MOMENT COEFFICIENT ERROR, SLOTTED WALL
F = 1.1844

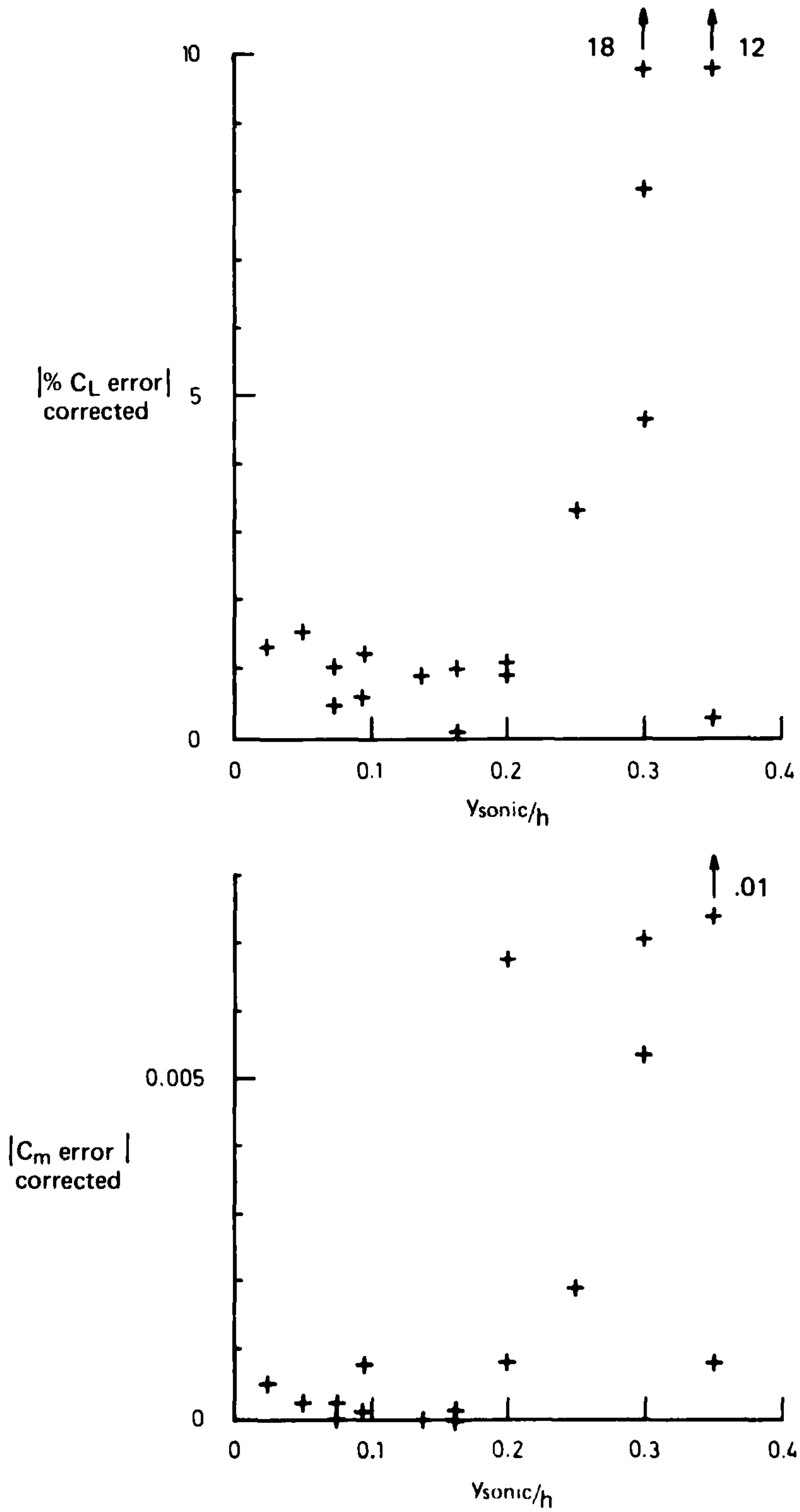

FIG. 19 CORRELATION OF SUPERCRITICAL SLOTTED WALL (F = 1.1844) INTERFERENCE

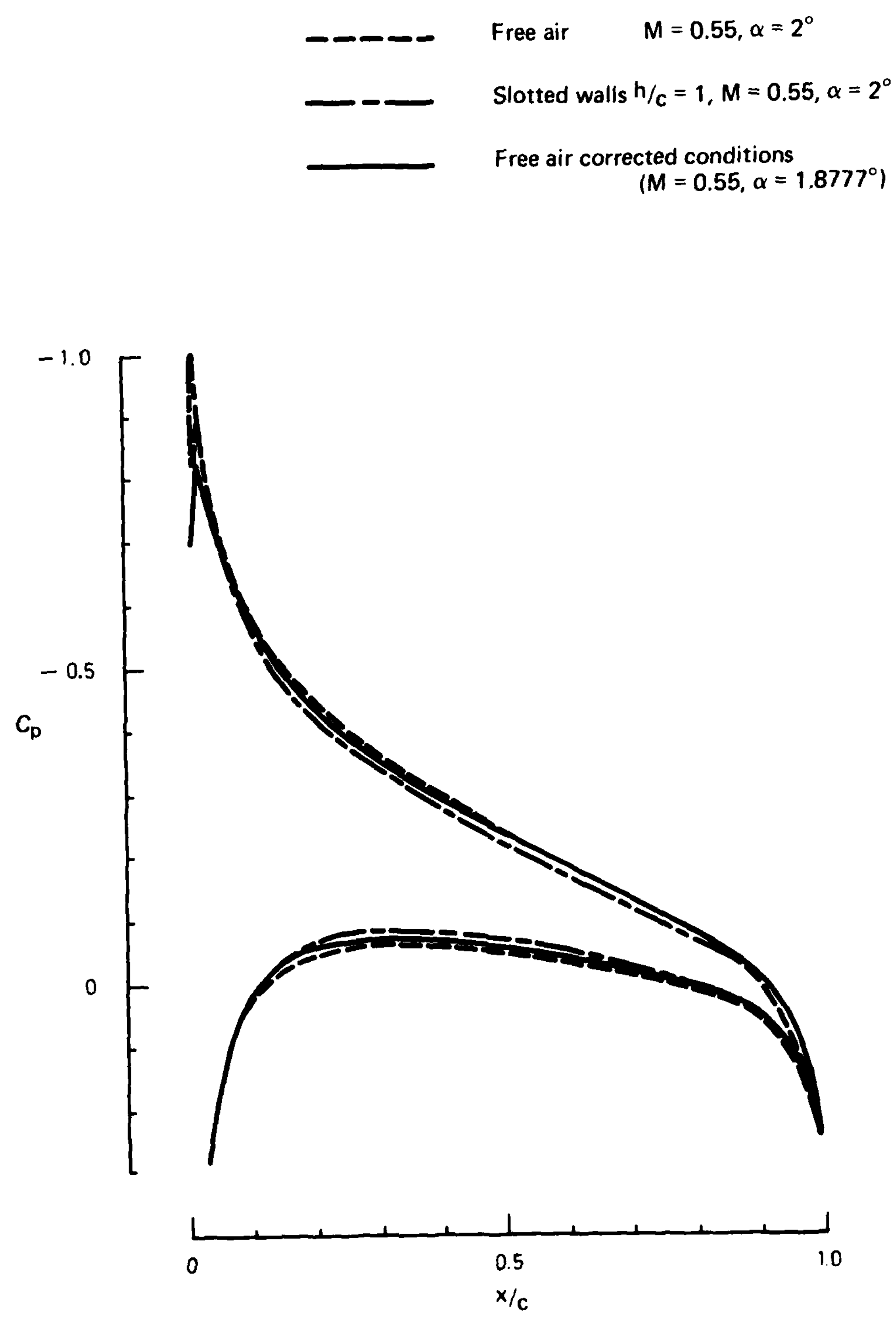

FIG. 20 PRESSURE DISTRIBUTIONS – NACA 0006
SLOTTED WALLS (F = 1.1844) AND FREE AIR

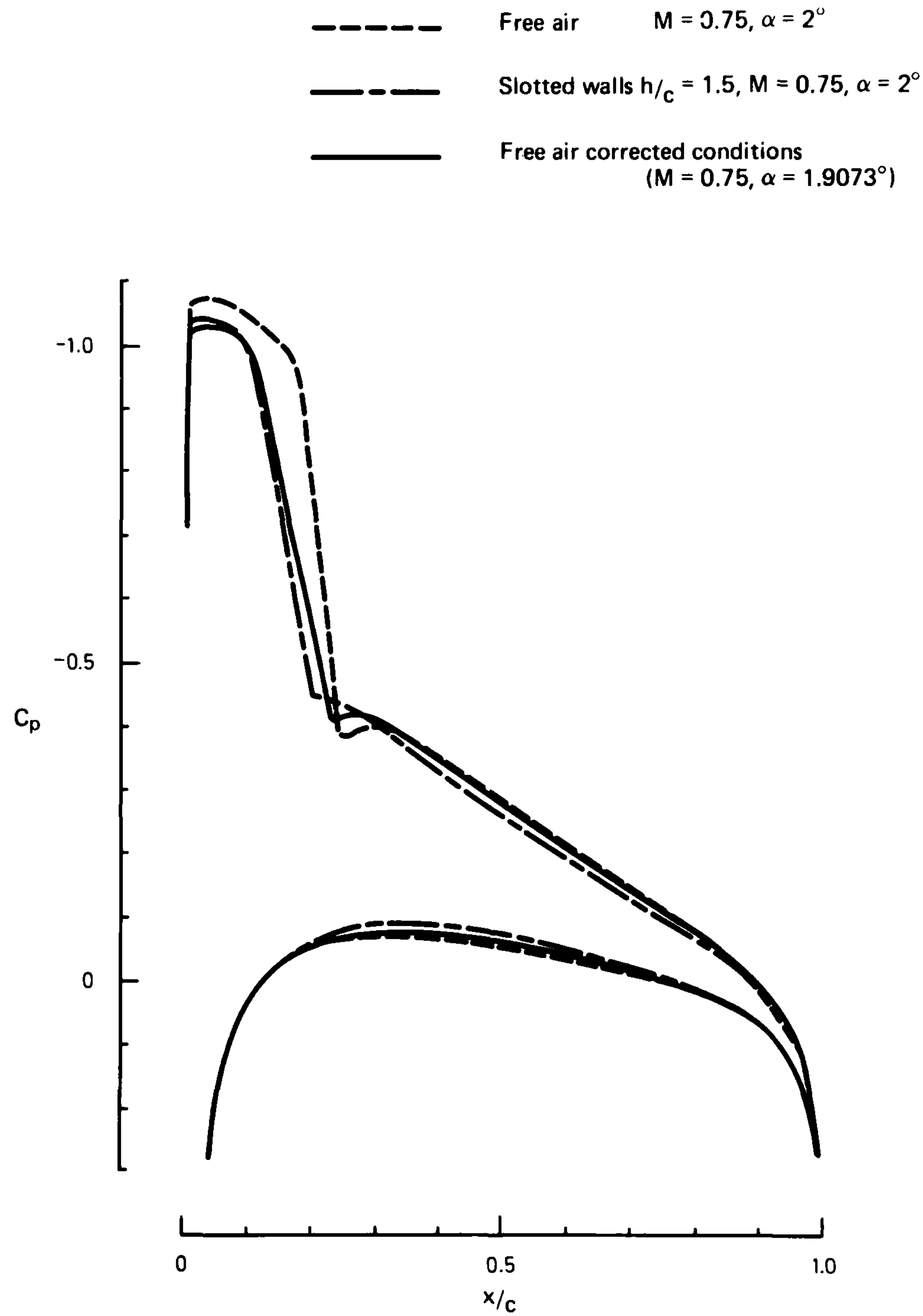

FIG. 21 PRESSURE DISTRIBUTIONS – NACA 0006
SLOTTED WALLS (F = 1.1844) AND FREE AIR

APPENDIX

Computed Results

Tunnel walls	Aerofoil section	Tunnel values h/c	M	α	C_L	C_m	C_D	Corrected values M_c	α_c	C_{L_c}	C_{m_c}	Free air values at corrected M and α C_L	C_m
Free air	NACA 0006	—	0·55	2·0	0·3104	0·00044	0						
Solid	NACA 0006	8	0·55	2·0	0·3139	0·00105	0	0·5504	2·0112	0·3121	0·00141	0·3121	0·00044
Solid	NACA 0006	4	0·55	2·0	0·3245	−0·00098	0	0·5515	2·0450	0·3172	0·00051	0·3176	0·00046
Solid	NACA 0006	3	0·55	2·0	0·3342	−0·00231	0	0·5526	2·0811	0·3208	0·00043	0·3234	0·00048
Solid	NACA 0006	2	0·55	2·0	0·3599	−0·00541	0	0·5558	2·1899	0·3278	0·00121	0·3409	0·00053
Solid	NACA 0006	1·5	0·55	2·0	0·3933	−0·00907	0	0·5604	2·3563	0·3318	0·00371	0·3677	0·00064
Solid	NACA 0006	1·0	0·55	2·0	0·4770	−0·01739	0	0·5734	2·9147	0·3150	0·01663	0·4589	0·00121
Free air	NACA 0012	—	0·55	2·0	0·3181	0·00026	0						
Solid	NACA 0012	8	0·55	2·0	0·3221	0·00082	0	0·5508	2·0144	0·3199	0·00118	0·3201	0·00026
Solid	NACA 0012	4	0·55	2·0	0·3341	−0·00126	0	0·5531	2·0462	0·3251	0·00028	0·3261	0·00028
Solid	NACA 0012	2	0·55	2·0	0·3759	−0·00612	0	0·5622	2·1973	0·3363	0·00078	0·3524	0·00036
Solid	NACA 0012	1·5	0·55	2·0	0·4174	−0·01039	0	0·5717	2·3751	0·3412	0·00309	0·3837	0·00051
Free air	NACA 0012	—	0·55	4·0	0·6398	0·00219	0						
Solid	NACA 0012	8	0·55	4·0	0·6479	0·00312	0	0·5508	4·0232	0·6434	0·00386	0·6440	0·00226
Solid	NACA 0012	4	0·55	4·0	0·6735	−0·00054	0	0·5532	4·0942	0·6551	0·00254	0·6569	0·00257
Solid	NACA 0012	3	0·55	4·0	0·6973	−0·00308	0	0·5556	4·1709	0·6637	0·00259	0·6707	0·00290
Solid	NACA 0012	2	0·55	4·0	0·7642	−0·00927	0	0·5626	4·4081	0·6828	0·00464	0·7138	0·00391
Free air	12%	—	0·55	2·0	0·3158	−0·00324	0						
Solid	Parabolic arc	4	0·55	2·0	0·3312	−0·00500	0	0·5530	2·0437	0·3223	−0·00345	0·3232	−0·00337
Solid	Parabolic arc	2	0·55	2·0	0·3715	−0·01071	0	0·5619	2·1845	0·3326	−0·00374	0·3475	−0·00380
Solid	Parabolic arc	1·5	0·55	2·0	0·4107	−0·01594	0	0·5711	2·3462	0·3363	−0·00234	0·3756	−0·00431
Free air	NACA 0006	—	0·75	2·0	0·3946	0·00548	0·00078						
Solid	NACA 0006	8	0·75	2·0	0·4081	0·00535	0·00077	0·7511	2·0190	0·4044	0·00609	0·4031	0·00575
Solid	NACA 0006	4	0·75	2·0	0·4478	0·00366	0·00131	0·7543	2·0819	0·4314	0·00690	0·4224	0·00661
Solid	NACA 0006	3	0·75	2·0	0·497611	0·001541	0·00246	0·7579	2·1587	0·4653	0·00793	0·4472	0·00752
Solid	NACA 0006	2·4	0·75	2·0	0·6082	0·011417	0·00715	0·7633	2·2768	0·5461	0·00097	0·4908	0·00821
Solid	NACA 0006	2·2*	0·75	2·0	0·8750	−0·113956	0·02829						

* Choked

APPENDIX—continued

Computed Results

Tunnel walls	Aerofoil section	Tunnel values						Corrected values				Free air values at corrected M and α	
		h/c	M	α	C_L	C_m	C_D	M_c	α_c	C_{L_c}	C_{m_c}	C_L	C_m
Free air	NACA 0012	—	0·75	2·0	0·5455	−0·01572	0·01406						
Solid	NACA 0012	8	0·75	2·0	0·5933	−0·02675	0·01775	0·7534	2·0215	0·5855	−0·02551	0·5865	−0·02549
Solid	NACA 0012	6	0·75	2·0	0·6518	−0·04313	0·02293	0·7561	2·0377	0·6367	−0·04058	0·6233	−0·03537
Solid	NACA 0012	4*	0·75	2·0	1·0047	−0·20337	0·06030	0·7630	2·0339	0·9539	−0·19171	0·7367	−0·07428
Free air	NACA 0012	—	0·70	2·0	0·3884	0·00356	0·00055						
Solid	NACA 0012	8	0·70	2·0	0·3996	0·00382	0·00047	0·7016	2·0170	0·3958	0·00443	0·3939	0·00376
Solid	NACA 0012	6	0·70	2·0	0·4084	0·00311	0·00063	0·7029	2·0307	0·4016	0·00422	0·3984	0·00392
Solid	NACA 0012	4	0·70	2·0	0·4338	0·00149	0·00105	0·7065	2·0722	0·4176	0·00417	0·4125	0·00436
Solid	NACA 0012	3	0·70	2·0	0·4770	−0·00123	0·00245	0·7116	2·1377	0·4454	0·00402	0·4361	0·00479
Solid	NACA 0012	2·4	0·70	2·0	0·5696	−0·01063	0·00675	0·7189	2·2403	0·5108	−0·00064	0·4776	0·00446
Free air	NACA 0006	—	0·75	3·0	0·6706	0·00156	0·01066						
Solid	NACA 0006	8	0·75	3·0	0·7039	0·00798	0·01194	0·7519	3·0326	0·6964	0·00924	0·6933	−0·001614
Solid	NACA 0006	6	0·75	3·0	0·7457	−0·00345	0·01414	0·7533	3·0576	0·7318	−0·00101	0·7118	−0·00453
Solid	NACA 0006	4	0·75	3·0	0·9458	−0·06772	0·02775	0·7583	3·1196	0·9051	−0·05992	0·7836	−0·019241
Free air	NACA 0006	—	0·55	2·0	0·3104	0·00044	0						
Open jet	NACA 0006	8	0·55	2·0	0·2471	0·00162	0	0·5498	1·5399	0·2495	0·00105	0·2388	0·00026
Open jet	NACA 0006	4	0·55	2·0	0·2003	0·00201	0	0·5493	1·2243	0·2081	0·00016	0·1897	0·00018
Open jet	NACA 0006	3	0·55	2·0	0·1757	0·00276	0	0·5487	1·0677	0·1880	−0·00013	0·1654	0·00015
Open jet	NACA 0006	2	0·55	2·0	0·1384	0·00434	0	0·5471	0·8336	0·1602	−0·00077	0·1290	0·00011
Open jet	NACA 0006	1·5	0·55	2·0	0·1122	0·00560	0	0·5448	0·6597	0·1438	−0·00178	0·1020	0·00008
Open jet	NACA 0006	1	0·55	2·0	0·0793	0·00690	0	0·5383	0·3838	0·1305	−0·00496	0·0592	0·00005
Free air	NACA 0006	—	0·75	2·0	0·3946	0·00548	0·00078						
Open jet	NACA 0006	8	0·75	2·0	0·2874	0·00351	0	0·7495	1·4587	0·2919	0·00246	0·2830	0·00169
Open jet	NACA 0006	4	0·75	2·0	0·2180	0·00393	0	0·7479	1·1365	0·2316	0·00073	0·2183	0·00058
Open jet	NACA 0006	3	0·75	2·0	0·1849	0·00496	0	0·7463	0·9881	0·2055	0·00013	0·1888	0·00033
Open jet	NACA 0006	2·5	0·75	2·0	0·1590	0·00597	0	0·7442	0·8707	0·1869	−0·00052	0·1654	0·00020

* Choked

APPENDIX—contiuued

Computed Results

Tunnel walls	Aerofoil section	Tunnel values						Corrected values				Free air values at corrected M and α	
		h/c	M	α	C_L	C_m	C_D	M_c	α_c	C_{L_c}	C_{m_c}	C_L	C_m
Free air	NACA 0012	—	0·77	2·0	0·9019	−0·14525	0·05035						
Open jet	NACA 0012	8	0·77	2·0	0·3872	−0·01194	0·01422	0·7688	1·2756	0·3941	−0·01349	0·3814	−0·01388
Open jet	NACA 0012	6	0·77	2·0	0·3308	−0·00462	0·01112	0·7678	1·1594	0·3413	−0·00696	0·3310	−0·00803
Open jet	NACA 0012	4	0·77	2·0	0·2545	0·00317	0·00740	0·7651	0·9906	0·2727	−0·00085	0·2635	−0·00225
Open jet	NACA 0012	3	0·77	2·0	0·2046	0·00695	0·00540	0·7612	0·8712	0·2309	0·00123	0·2183	0·00035
Open jet	NACA 0012	2	0·77	2·0	0·1443	0·00979	0·00305	0·7503	0·6966	0·1868	0·00069	0·1575	0·00150
Free air	NACA 0006	—	0·55	2·0	0·3104	0·00044	0						
Porous. 3 P 0·78	NACA 0006	8	0·55	2·0	0·2726	0·00114	0	0·5499	1·7189	0·2727	0·001138	0·2666	0·00032
Porous. 3 P 0·78	NACA 0006	4	0·55	2·0	0·2448	−0·00006	0	0·5497	1·4950	0·2451	−0·00006	0·2318	0·00025
Porous. 3 P 0·78	NACA 0006	3	0·55	2·0	0·2302	−0·00067	0	0·5494	1·3668	0·2306	−0·00067	0·2119	0·00022
Free air	NACA 0006	—	0·55	2·0	0·3104	0·00044	0						
Sl. wall. F 1·59.	NACA 0006	8	0·55	2·0	0·3111	0·00140	0	0·5500	2·0	0·3110	0·00140	0·3104	0·00044
Sl. wall. F 1·59.	NACA 0006	6	0·55	2·0	0·3116	0·00093	0	0·5501	2·0	0·3116	0·00093	0·3104	0·00044
Sl. wall. F 1·59.	NACA 0006	4	0·55	2·0	0·3120	0·00048	0	0·5501	2·0	0·3119	0·00048	0·3104	0·00044
Sl. wall. F 1·59.	NACA 0006	3	0·55	2·0	0·3117	0·00031	0	0·5502	2·0	0·3115	0·00031	0·3104	0·00044
Sl. wall. F 1·59.	NACA 0006	2	0·55	2·0	0·3091	0·00052	0	0·5505	2·0	0·3087	0·00051	0·3105	0·00044
Sl. wall. F 1·59.	NACA 0006	1·5	0·55	2·0	0·3032	0·00132	0	0·5508	2·0	0·3025	0·00132	0·3106	0·00044
Sl. wall. F 1·59.	NACA 0006	1	0·55	2·0	0·2816	0·00426	0	0·5518	2·0	0·2801	0·00423	0·3108	0·00044
Sl. wall. F 1·59.	NACA 0006	0·6	0·55	2·0	0·2230	0·01077	0	0·5551	2·0	0·2198	0·01061	0·3116	0·00044
Free air	NACA 0006	—	0·75	2·0	0·3946	0·00548	0·00078						
Sl. wall. F 1·59.	NACA 0006	8	0·75	2·0	0·4002	0·00600	0·00063	0·7501	2·0	0·4001	0·00600	0·3946	0·00548
Sl. wall. F 1·59.	NACA 0006	4	0·75	2·0	0·4021	0·00579	0·00075	0·7503	2·0	0·4018	0·00579	0·3948	0·00548
Sl. wall. F 1·59.	NACA 0006	3	0·75	2·0	0·4015	0·00627	0·00076	0·7506	2·0	0·4011	0·00626	0·3950	0·00548
Sl. wall. F 1·59.	NACA 0006	2	0·75	2·0	0·3919	0·00701	0·00064	0·7513	2·0	0·3910	0·00700	0·3955	0·00549
Sl. wall. F 1·59.	NACA 0006	1·5	0·75	2·0	0·3727	0·00894	0·00050	0·7523	2·0	0·3712	0·00891	0·3962	0·00550
Sl. wall. F 1·59.	NACA 0006	1	0·75	2·0	0·3193	0·01344	0·00027	0·7552	2·0	0·3164	0·01332	0·3982	0·00553

APPENDIX—continued

Computed Results

Tunnel walls	Aerofoil section	Tunnel values						Corrected values				Free air values at corrected M and α	
		h/c	M	α	C_L	C_m	C_D	M_c	α_c	C_{Lc}	C_{mc}	C_L	C_m
Free air . . .	NACA 0006 .	—	0·55	2·0	0·3104	0·00044	0						
Sl. wall, F 1·1844	NACA 0006 .	8	0·55	2·0	0·3105	0·00147	0	0·55	1·9979	0·3108	0·00140	0·3100	0·00044
Sl. wall, F 1·1844	NACA 0006 .	4	0·55	2·0	0·3036	0·00075	0	0·55	1·9916	0·3107	0·00048	0·3091	0·00043
Sl. wall, F 1·1844	NACA 0006 .	3	0·55	2·0	0·3076	0·00079	0	0·55	1·9852	0·3095	0·00031	0·3081	0·00043
Sl. wall, F 1·1844	NACA 0006 .	2	0·55	2·0	0·3007	0·00148	0	0·55	1·9671	0·3049	0·00042	0·3053	0·00043
Sl. wall, F 1·1844	NACA 0006 .	1·5	0·55	2·0	0·2899	0·00277	0	0·55	1·9426	0·2972	0·00095	0·3015	0·00042
Sl wall, F 1·1844	NACA 0006 .	1	0·55	2·0	0·2601	0·00629	0	0·55	1·8777	0·2747	0·00263	0·2914	0·00041
Free air . . .	NACA 0006 .	—	0·75	2·0	0·3946	0·00548	0·00078						
Sl wall, F 1·1844	NACA 0006 .	8	0·75	2·0	0·3985	0·00610	0·00060	0·75	1·9964	0·3991	0·00596	0·3939	0·00547
Sl wall, F 1·1844	NACA 0006 .	4	0·75	2·0	0·3955	0·00621	0·00064	0·75	1·9858	0·3977	0·00565	0·3918	0·00544
Sl wall, F 1·1844	NACA 0006 .	3	0·75	2·0	0·3896	0·00657	0·00058	0·75	1·9750	0·3935	0·00560	0·3897	0·00541
Sl wall, F 1·1844	NACA 0006 .	2	0·75	2·0	0·3708	0·00821	0·00057	0·75	1·9454	0·3791	0·00613	0·3838	0·00533
Sl wall, F 1·1844	NACA 0006 .	1·5	0·75	2·0	0·3436	0·01041	0·00033	0·75	1·9073	0·3574	0·00698	0·3763	0·00522
Sl wall, F 1·1844	NACA 0006 .	1	0·75	2·0	0·2833	0·01464	0·00014	0·75	1·8149	0·3088	0·00829	0·3581	0·00497
Free air . . .	NACA 0012 .	—	0·55	2·0	0·3181	0·00026	0						
Sl wall, F 1·1844	NACA 0012 .	8	0·55	2·0	0·3181	0·00125	0	0·55	1·9978	0·3184	0·00118	0·3177	0·00026
Sl wall, F 1·1844	NACA 0012 .	4	0·55	2·0	0·3173	0·00059	0	0·55	1·9914	0·3184	0·00031	0·3167	0·00025
Sl wall, F 1·1844	NACA 0012 .	3	0·55	2·0	0·3152	0·00064	0	0·55	1·9849	0·3171	0·00015	0·3157	0·00025
Sl wall, F 1·1844	NACA 0012 .	2	0·55	2·0	0·3078	0·00138	0	0·55	1·9664	0·3121	0·00029	0·3127	0·00025
Sl wall, F 1·1844	NACA 0012 .	1·5	0·55	2·0	0·2963	0·00274	0	0·55	1·9415	0·3037	0·00089	0·3088	0·00025
Sl wall, F 1·1844	NACA 0012 .	1	0·55	2·0	0·2645	0·00644	0	0·55	1·8756	0·2794	0·00271	0·2983	0·00024
Free air . . .	NACA 0012 .	—	0·75	2·0	0·5455	−0·01572	0·10406						
Sl wall, F 1·1844	NACA 0012 .	8	0·75	2·0	0·5461	−0·01520	0·01385	0·75	1·9959	0·5469	−0·01539	0·5438	−0·01551
Sl wall, F 1·1844	NACA 0012 .	4	0·75	2·0	0·5406	−0·01428	0·01371	0·75	1·9836	0·5437	−0·01504	0·5387	−0·01486
Sl wall, F 1·1844	NACA 0012 .	3	0·75	2·0	0·5283	−0·01204	0·01314	0·75	1·9711	0·5335	−0·01336	0·5332	−0·01418
Sl wall, F 1·1844	NACA 0012 .	2	0·75	2·0	0·4843	−0·00444	0·01065	0·75	1·9369	0·4952	−0·00716	0·5194	−0·01260
Sl wall, F 1·1844	NACA 0012 .	1·5	0·75	2·0	0·4246	0·00468	0·00783	0·75	1·8933	0·4416	0·00044	0·5024	−0·01077
Sl wall, F 1·1844	NACA 0012 .	1	0·75	2·0	0·3143	0·01687	0·00334	0·75	1·7933	0·3425	0·00982	0·4646	−0·00714

APPENDIX—continued

Computed Results

Tunnel walls	Aerofoil section	Tunnel values						Corrected values				Free air values at corrected M and α	
		h/c	M	α	C_L	C_m	C_D	M_c	α_c	C_{Lc}	C_{mc}	C_L	C_m
Free air . . .	NACA 0006 .	—	0·75	3·0	0·6706	0·00156	0·01066						
Sl. wall, $F = 1\cdot1844$	NACA 0006 .	8	0·75	3·0	0·6714	0·01202	0·01033	0·75	2·9939	0·6724	0·01179	0·6692	0·00156
Sl. wall, $F = 1\cdot1844$	NACA 0006 .	4	0·75	3·0	0·6645	0·00338	0·01005	0·75	2·9771	0·6683	0·00245	0·6628	0·00238
Sl. wall, $F = 1\cdot1844$	NACA 0006 .	3	0·75	3·0	0·6551	0·01142	0·01025	0·75	2·9579	0·6616	0·00979	0·6562	0·00302
Sl. wall, $F = 1\cdot1844$	NACA 0006 .	2	0·75	3·0	0·6095	0·01643	0·00831	0·75	2·9086	0·6232	0·01301	0·6442	0·01116
Sl. wall, $F = 1\cdot1844$	NACA 0006 .	1·5	0·75	3·0	0·5503	0·02180	0·00610	0·75	2·8466	0·5723	0·01631	0·6214	0·00936
Sl. wall, $F = 1\cdot1844$	NACA 0006 .	1	0·75	3·0	0·4357	0·02823	0·00309	0·75	2·7030	0·4748	0·01846	0·5776	0·01142
Free air . .	NACA 0012 .	—	0·78	2·0	0·9733	−0·19673	0·05973						
Sl. wall, $F = 1\cdot1844$	NACA 0012 .	8	0·78	2·0	0·9715	−0·19638	0·05922	0·78	1·9983	0·9730	−0·19676	0·9730	−0·19670
Sl. wall, $F = 1\cdot1844$	NACA 0012 .	4	0·78	2·0	0·9638	−0·19427	0·05972	0·78	1·9933	0·9699	−0·19578	0·9723	−0·19659
Sl. wall, $F = 1\cdot1844$	NACA 0012 .	3	0·78	2·0	0·9607	−0·19070	0·06041	0·78	1·9874	0·9714	−0·19333	0·9715	−0·19646
Sl. wall, $F = 1\cdot1844$	NACA 0012 .	2	0·78	2·0	0·8171	−0·12395	0·04756	0·78	1·9540	0·8375	−0·12907	0·9667	0·19578
Sl. wall, $F = 1\cdot1844$	NACA 0012 .	1·5	0·78	2·0	0·5988	−0·04740	0·02787	0·78	1·8960	0·6254	−0·05407	0·9583	−0·19463
Sl. wall, $F = 1\cdot1844$	NACA 0012 .	1	0·78	2·0	0·3612	0·00825	0·01068	0·78	1·7744	0·3975	−0·00080	0·8928	−0·17138

DISTRIBUTION

	Copy No.
AUSTRALIA	
DEPARTMENT OF DEFENCE	
Central Office	
Chief Defence Scientist	1
Deputy Chief Defence Scientist	2
Superintendent, Science and Technology Programs	3
Australian Defence Scientific and Technical Representative (UK)	
Counsellor, Defence Science (USA)	
Defence Central Library	4
Document Exchange Centre, DISB	5-21
Joint Intelligence Organisation	22
Aeronautical Research Laboratories	
Chief Superintendent	23
Library	24
Superintendent—Aerodynamics	25
Divisional File—Aerodynamics	26
Author: N. Pollock	27
Transonic Wind Tunnel	28
Materials Research Laboratories	
Library	29
Defence Research Centre	
Library	30
Central Office	
Director-General—Army Development (NSO)	31-34
Engineering Development Establishment	
Library	35
RAN Research Laboratory	
Library	36
Navy Office	
Naval Scientific Adviser	37
Army Office	
Army Scientific Adviser	38
Royal Military College Library	39
Air Force Office	
Aircraft Research and Development Unit, Scientific Flight Group	40
Air Force Scientific Adviser	41
Technical Division Library	42
HQ Support Command (SESO)	43
RAAF Academy, Point Cook	44

DEPARTMENT OF INDUSTRY AND COMMERCE

Government Aircraft Factories, Library	45

STATUTORY AND STATE AUTHORITIES AND INDUSTRY

SEC of Victoria, Herman Research Laboratory, Library	46
Commonwealth Aircraft Corporation, Library	47

UNIVERSITIES AND COLLEGES

Adelaide	Barr Smith Library	48
Melbourne	Engineering Library	49
Monash	Hargrave Library	50
Newcastle	Library	51
Sydney	Engineering Library	52
Queensland	Library	53
Tasmania	Engineering Library	54
Western Australia	Library	55
RMIT	Library	56

CANADA

NRC, Aeronautical and Mechanical Engineering Library	57

FRANCE

ONERA, Library	58

GERMANY

Fachinformationszentrum: Energie, Physik, Mathematik G.m.b.H.	59

INDIA

National Aeronautical Laboratory, Information Centre	60

ISRAEL

Technion-Israel Institute of Technology, Professor J. Singer	61

NETHERLANDS

National Aerospace Laboratory (NLR), Library	62

SWEDEN

Aeronautical Research Institute, Library	63

UNITED KINGDOM

CAARC, Secretary (NPL)	64
Royal Aircraft Establishment	
Farnborough, Library	65
Bedford, Library	66
British Library, Lending Division	67
Aircraft Research Association, Library	68

UNITED STAES OF AMERICA

NASA Scientific and Technical Information Facility	69
The John Crerar Library	70

Spares (10)	71 80

END

DATE
FILME

04-8

DTIC